DOKUZ EYLÜL UNIVERSITY

GRADUATE SCHOOL OF NATURAL AND APPLIED SCIENCES

GEOTECHNICAL CHARACTERIZATION OF NATURAL ZEOLITE

by

Tuğçe ÖZDAMAR

August 2012

İZMİR

GEOTECHNICAL CHARACTERIZATION OF NATURAL ZEOLİTE

A Thesis Submitted to the

Graduate School of Natural and Applied Sciences of Dokuz Eylül University

In Partial Fulfillment of the Requirements for the Degree of Master of Sciencie
in

Civil Engineering, Applied Geotechnical Program

Tuğçe ÖZDAMAR

August 2012

İZMİR

M.Sc THESIS EXAMINATION RESULT FORM

We have read the thesis entitled **"GEOTECHNICAL CHARACTERIZATION OF NATURAL ZEOLITE"** completed by **TUĞÇE ÖZDAMAR** under supervision of **ASSIST.PROF.A. HAKAN ÖREN** and we certify that in our opinion it is fully adequate, in scope and in quality, as a thesis for the degree of Master of Science.

Assist.Prof.A. Hakan ÖREN

Supervisor

Prof.Dr.Arif Ş. KAYALAR

(Jury Member)

Prof.Dr.M. Yalçın KOCA

(Jury Member)

Prof.Dr. Mustafa SABUNCU
Director

Graduate School of Natural and Applied Sciences

ACKNOWLEDMENTS

I would like to present my sincere gratitude to my advisor, Assist.Prof.A. Hakan Ören for his guidance throughout my period of thesis. I am really appreciated to him for his technical and mental supports from the beginning of graduate school life. His intellectual contributions, patience and guidance have always increased my experience and encouraged me to be better.

I would also like to thank Prof.Dr.Arif Ş. Kayalar for his professional guidance and contributions in my thesis. Additionally, I would like to thank Research Assistant of Soil Mechanics Division of Civil Engineering Department, Fatih Işık and Gökhan İmançlı for expanding my understanding of soil mechanics. I would also like to many thanks my friends Uğur Ülgen, Oya Özlem Dinçsoy and Şafak Söylemez for their helps. They are always near me whenever I need.

I would like to acknowledge to my family, especially my mother. She has always supported, helped and encouraged me with her eternal love and patience throughout my life. I have never forgotten their contributions.

At last but not least, I would like to thank Oğuz Kul who has never left me alone and accompanied me patiently during my study. Special thanks for his contributions, existence and happiness to be in my life.

GEOTECHNICAL CHARACTERIZATION OF NATURAL ZEOLITE

ABSTRACT

This study covers the findings of laboratory test results on two different zeolites. During the laboratory tests, different grain sized zeolites were used. According to the present fine contents, zeolites were entitled with “granular” (GZ-1 and GZ-2) and “fine” (FZ-1 and FZ-2).

Most of the previous studies on zeolites were focused on the cation exchange capacities (CECs) of the material. The alternative usage of zeolite with bentonite instead of sands has also been investigated. However, a study on the use of zeolites alone in geotechnical applications has not been investigated, so far.

In this thesis, geotechnical characterization of natural zeolites was presented. To assess the suitability of zeolites in geotechnical applications, some engineering properties of zeolites (e.g., compaction properties, compressibility, shear strength and hydraulic conductivity) were investigated.

The results show that zeolites had relatively low dry unit weights than those of sands and clays. Also, it is observed that the shear strength properties of zeolites were similar with dense sands. Hydraulic conductivity tests showed that the compacted granular and fine zeolites have high hydraulic conductivities than the desired limit values for impervious soil liners. Based on the obtained results, it is concluded that zeolites may be used as a light weight geomaterial and permeable reactive barrier material in many geotechnical applications.

Keywords: compacted zeolites, grain size, hydraulic conductivity, zeolite

DOĞAL ZEOLİTİN GEOTEKNİK KARAKTERİZASYONU

ÖZ

Bu çalışma iki farklı zeolit üzerinde gerçekleştirilen laboratuar deneylerini kapsamaktadır. Laboratuar deneyleri sırasında farklı dane boyutlarında zeolitler kullanılmıştır. Zeolitler içerdikleri ince dane miktarına göre "iri" (GZ-1 ve GZ-2) ve "ince" (FZ-1 ve FZ-2) olarak isimlendirilmişlerdir.

Zeolitler üzerinde daha önce yapılmış olan birçok çalışma zeolitin katyon değişim kapasitesi (KDK) üzerinde odaklanmıştır. Zeolitin kum yerine bentonit ile birlikte kullanımı da ayrıca araştırılmıştır. Ancak, zeolitlerin geoteknik uygulamalarda tek başına kullanılmasını inceleyen bir çalışma bu güne kadar yapılmamıştır.

Bu tezde, doğal zeolitlerin geoteknik karakterizasyonuna yönelik bir çalışma sunulmaktadır. Zeolitlerin geoteknik uygulamalarda kullanılabilirliğinin değerlendirilmesi amacı ile zeolitlerin bazı mühendislik özellikleri (örneğin, sıkıştırma özellikleri, sıkışabilirliği, kayma dayanımı ve hidrolik iletkenliği) incelenmiştir.

Deney sonuçları zeolitin kum ve killerinkinden nisbeten daha düşük kuru birim hacim ağırlıklara sahip olduğunu göstermiştir. Ayrıca, zeolitlerin kayma dayanımlarının sıkı kumlarınkine benzer olduğu gözlemlenmiştir. Hidrolik iletkenlik deneyleri, sıkıştırılmış iri ve ince zeolitlerin hidrolik iletkenliklerinin geçirimsiz dolgu malzemelerinin sağlaması gereken sınır değerden daha yüksek olduğunu göstermiştir. Elde edilen sonuçlara dayanarak zeolitin düşük ağırlıklı zemin malzemesi ve geçirimli reaktif bariyer malzemesi olarak kullanılabileceği sonucuna varılmıştır.

Anahtar sözcükler: sıkıştırılmış zeolit, dane boyu, hidrolik iletkenlik, zeolit

CONTENTS

Page

CHAPTER ONE
INTRODUCTION

1.1 Introduction

Zeolites are hydrated aluminosilicates of alkali and alkaline earth metals with unique crystal structures consisting of a three-dimensional framework of SiO_4 and AlO_4 (Kayabalı, 1997). The isomorphous substitution of Si^{4+} by Al^{3+} produces a negative charge in the lattice (Blanchard, Maunaye & Martin, 1984). Since zeolites can be found abundantly in many parts of the world, especially in Turkey, their construction costs are effectively the same as sand in terms of to their availability.

Zeolite has been used as permeable reactive barriers to control the contaminant transportation during the last two decades. Since zeolite has negatively charged surface and high cation exchange capacity, researchers suggest that zeolite-bentonite mixtures can alternatively be used in place of sand-bentonite mixtures in landfill liner applications. Despite beneficial use of zeolites and zeolite-bentonite mixtures, there is little information on the geotechnical characterization of zeolite. This study shows some basic geotechnical characteristics of clinoptilolite rich zeolites.

In this regard, this thesis presents the detailed results of the laboratory tests for the geotechnical characterization of four natural zeolites. For this purpose, zeolites gathered from two different sources in Gördes were tested. Two zeolites had larger and uniform (i.e. namely GZ-1, GZ-2) while other two zeolites had finer and well-graded (i.e. namely FZ-1, FZ-2) particle size distribution.

This thesis consists of six chapters. Chapter one outlines the general overview and the scope of this study and organization of the thesis.

The extended literature review is given in Chapter two. In this chapter general information about zeolite and its applications are summarized.

Chapter three describes the material characterization and experimental procedures which are followed in this study.

Chapter four discusses the compaction, consolidation, shear strength and hydraulic conductivity test results.

Chapter five presents the conclusions and recommendations for future studies based on the results obtained from this study.

CHAPTER TWO
LITERATURE REVIEW

2.1 General Information About Zeolite Properties

Since their discovery in saline-lake deposits of Tertiary in the western United States in 1756, zeolites get a large using area in the world because of the unique physical and chemical properties (Köktürk, 1995).

Zeolites are microporous, hydrated aluminasilicates that can accommodate various cations such as Na^+, K^+, Ca^{2+}, Mg^{2+} and others. Their unique crystal structures form from three-dimensional framework of SiO_4 and AlO_4. Because of high cation exchange capacity, zeolites are used as wastewater and radioactive waste treatment media and filter material. The zeolites framework consists of uniformly sized pores of molecular dimensions (Maesen, 2007, chap. 1). Depending on the type of zeolite mineral, the pore size of the channels may vary from 2.5 to 5.0 Å (Koizumi & Roy, 1960). Three dimensional frameworks of aliminum tetrahedron and silisium tetrahedron are shown in Figure 2.1.

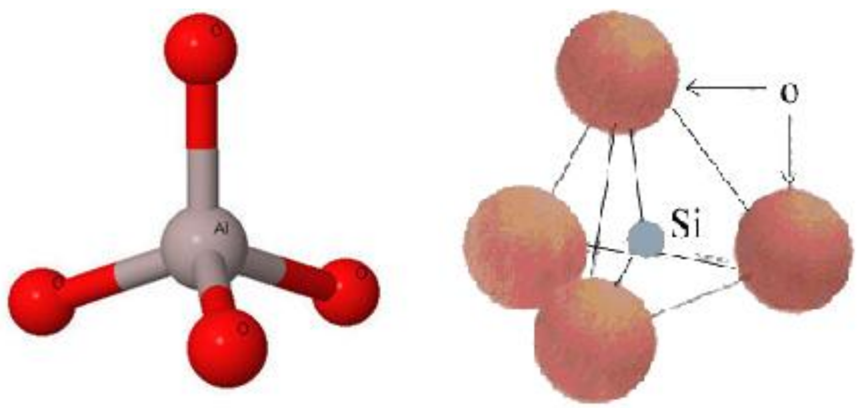

Figure 2.1 Three dimensional frameworks of aliminum tetrahedron (http://www.cmasc.gmu.edu/samp.htm) and silisium tetrahedron (http://www.crystalflame.com/en/crystal-healing-info/what-quartz-made/)

SiO_4 or AlO_4 are the smallest tetrahedra units of zeolite crystals. These smallest units are called as primary frame units. Secondary frame units and poliders are formed by the combination of these primary frame units. Differences between the poliders and secondary frame units or the connection types in three dimensions lead to formation of different zeolite crystals (Köktürk, 1995).

There are more than 40 different zeolite minerals exist in the nature (Trgo & Peric, 2003). However, only four types of them are mostly used in many applications due to their high cation exchange capacities (Jacobs & Förstner, 1999, Ören, Kaya & Kayalar, 2011):

- clinoptilolite, (Na_4K_5) $(Al_8Si_{40}O_{96}).24H_2O$
- chabazite, $(Na_2Ca)_6$ $(Al_{12}Si_{24}O_{72}).40H_2O$
- mordenite, $Na_8(Al_8Si_{40}O_{96}).24H_2O$
- phillipsite, $(NaK)_{10}(Al_{10}Si_{22}O_{64})20H_2O$

Honeycomb structures of mostly used two types of zeolites, clinoptiolite and mordenite, are shown in Figure 2.2.

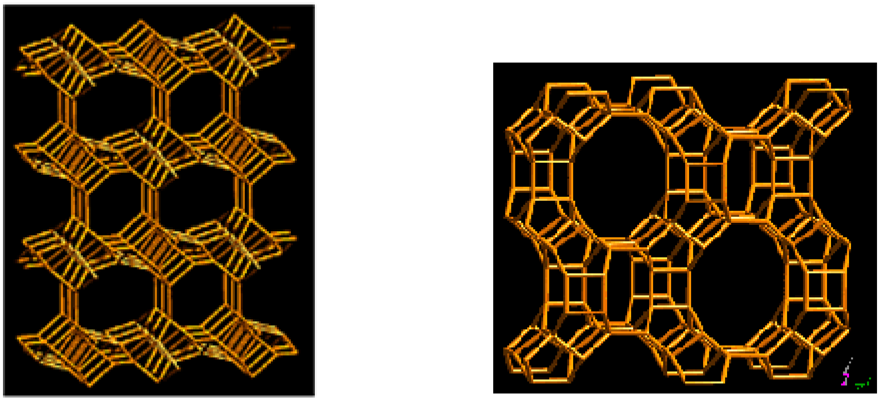

(a) (b)

Figure 2.2 Honeycomb structures of a) clinoptiolite (Koyama & Takeuchi, 1977) and b) mordenite (Koizumi & Roy, 1960)

Most occurrences of zeolites have been identified in sedimentary rocks of volcanic origin all over the world. Phillipsite and clinoptilolite are widely available in the deep-sea sediments and deposits of saline-alkaline lakes,. In these environments, mordenite rarely occurs, but commonly forms as alternative mineral in many geothermal areas (Kaçmaz & Köktürk, 2004). Natural zeolites occur in many locations of the world, e.g., in western USA, Turkey and Italy. Locations and associated mineral types in Turkey and in the world are given Table 2.1 and Table 2.2, respectively.

Generally, sedimentary zeolitic tuffs contain 50-95% of single zeolite. Also, they are soft, friable and light weighted. However, several zeolites may include volcanic glass, quartz, K-feldspar, montmorillonite, calcite, gypsum, and cristobalite/tridymite (Mumpton, 1999).

Table 2.1 Location of zeolite deposits by means of mineralogical origins in Turkey (Birsoy, 2002).

Deposits	**Associated Minerals**
Beypazarı	Clinoptilolite, analcime, saponite, K-feldspar, smectite, quartz, calcite
Yozgat	Clinoptilolite, smectite
Nevşehir (Cappadocia)	Erionite, chabazite, analcime, phillipsite, mordenite±clinoptilolite, smectite, quartz, opal-CT, K-feldspar
Kırka	Clinoptilolite, heulandite, analcime, calcite, opal-CT, smectite, quartz, K-feldspar
Emet	Clinoptilolite, analcime, opal-CT, K-feldspar, smectite, quartz, calcite
Şile	Mordenite, K-feldspar, opal-CT, quartz
Bigadiç	Clinoptilolite, heulandite, analcime, phillipsite, smectite, opal-CT, quartz, K-feldspar
Gördes	Clinoptilolite, heulandite, opal-CT, quartz, smectite
Keşan	Analcime, clinoptilolite, smectite, quartz, cristobalite, calcite

Table 2.2 Zeolite occurrences in the world (Köktürk, 1995, International Committee on Natural Zeolites 1984).

Continent	Country	Associated Minerals
Europe	Belgium	Laumontite
	Bulgaria	Clinoptilolite, Mordenite, Analcime, Natrolite
	Czechoslavakia	Clinoptilolite
	Denmark	Clinoptilolite
	Finland	Laumontite
	France	Clinoptilolite
	Germany	Chabazite
	England	Analcime, Clinoptilolite
	Hungary	Laumontite, Clinoptilolite, Mordenite
	Italy	Chabazite, Phillipsite, Analcime
	Poland	Clinoptilolite
	Romania	Clinoptilolite
	Muscovy	Clinoptilolite, Mordenite, Analcime, Chabazite
	Spain	Laumontite
	Swiss	Clinoptilolite, Mordenite
	Yugoslavia	Clinoptilolite, Analcime, Mordenite, Erionite
Africa	Angola	Clinoptilolite
	Botswana	Clinoptilolite
	Congo	Analcime
	Egypt	Heulandite
	Kenya	Phillipsite, Erionite
	Northern Africa	Analcime, Clinoptilolite, Mordenite
	Tanzania	Erionite, Chabazite, Phillipsite, Analcime, Clinoptilolite
Asia and Australia	Iran	Clinoptilolite
	Israel	Clinoptilolite
	Pakistan	Analcime
	Australia	Clinoptilolite
	China	Clinoptilolite
	Formosa	Clinoptilolite, Laumontite, Analcime
	Japan	Clinoptilolite, Mordenite, Laumontite, Analcime
	Korea	Clinoptilolite
	New Zealand	Clinoptilolite, Mordenite, Laumontite, Analcime
	Oceania	Laumontite, Clinoptilolite
South America	Argentine	Clinoptilolite, Laumontite, Analcime
	Chili	Clinoptilolite
North America	USA	Clinoptilolite, Chabazite, Erionite, Mordenite
	Canada	Laumontite, Clinoptilolite
	Cuba	Clinoptilolite, Mordenite
	Guatemala	Clinoptilolite
	Mexico	Clinoptilolite, Mordenite, Analcime, Erionite, Phillipsite
	Panama	Clinoptilolite
	West Indies	Wairakite, Clinoptilolite
Antarctica		Laumontite, Phillipsite

Zeolites are generally known as molecular sieves. Molecular sieve means the material property based primarily on size exclusion. Basically, small molecules can able to pass through entry channels, but larger ones excluded. The dimensions of the channels in zeolite crystals control the maximum particle size that will enter the pores. Furthermore, zeolites have high selectivity to adsorb polar molecules. The cation exchange capacity (CEC) of zeolite depends on the amount of Al that can replace with Si in the tetrahedral framework; the greater the Al content, the more extra framework cations needed to balance the charge (Mumpton, 1999).

CECs of natural zeolites are within the range of 2-4 milliequivalents/g (meq/g). Clinoptilolite which is the most common zeolite formation has a CEC 2.25 meq/g, and its cation exchange selectivity is; Cs > Rb > K > NH_4 > Ba > Sr >Na > Ca > Fe > Al > Mg > Li (Mumpton, 1999).

2.2 Literature Studies on Zeolites

As a result of high negative surface area and cation exchange capacity, zeolites could be used as permeable reactive barrier material (Lee et al., 2010). Also, some researchers suggested that, zeolite could be used as landfill liner material by mixing bentonite (Kayabalı, 1997).

2.2.1 Zeolite as Permeable Reactive Barrier (PRB)

Park et al. (2002) studied on the use of clinoptilolite as permeable reactive barriers (PRBs). They performed batch test and column test for the determination of the design factors of PRBs against the contaminated groundwater. Hydraulic conductivities (permeability) of the specimens with various particle sizes were determined in column tests using flexible-wall permeameters. Specimens were prepared by 10 times tamping the soil in the mould with three layers. The dimensions of the samples were 3 cm in diameter and 7 cm in height. The highest hydraulic conductivity was achieved at 20/80 ratio of 0.42-0.85 mm grain sized zeolite and Jumunjin sand mixtures. The obtained hydraulic conductivity values of the mixtures were in range 2×10^{-3} to 7×10^{-4} cm/s. However, the hydraulic conductivity of 100% zeolite (0-1 mm particle size) was obtained less than 1×10^{-6} cm/s. Also, the shear strength properties of Jumunjin sand and the mixtures were determined by using direct shear test in fully saturated conditions. The internal friction angles were obtained similar as 27.3° and 28.9° for Jumunjin sand and the mixtures with 20/80 ratio, respectively. The cohesion factor of the Jumunjin sand was obtained higher than the mixtures.

Lee et al. (2010) investigated the factors affecting the performance of zeolitic rock barrier as permeable reactive barriers. For this purpose several tests were conducted on three different sources (A, B and C) and three groups (1, 2 and 3) with different particle sized zeolites. Particle size ranges for three groups (1, 2 and 3) were 0.15-0.42, 0.42-0.84 and 0.84-2.00 mm, respectively. Falling head hydraulic conductivity tests were performed using rigid-wall glass column which has 2.4 cm diameter and 20 cm height. Samples were packed into the glass column to 1.0 g/cm^3 dry density. Hydraulic conductivity tests were performed with an average hydraulic gradient of 10 and DI water was used as the permeant. The authors reported that if the particle size decreased from 0.84-2.00 to 0.15-0.42 mm, the hydraulic conductivity decreased by approximately from 1×10^{-3} cm/s to 1×10^{-5} cm/s for samples A, B and C. The highest hydraulic conductivity was obtained from samples B, A and C with a different particle sizes. They also obtained that the hydraulic conductivity apparently affected from material type at the intermediate particle size (0.42-0.84 mm), but material type became insignificant at low (0.15-0.42 mm) or high (0.42-2.00 mm) particle size ranges.

Navia et al. (2005) investigated the possible use of volcanic soils as a landfill liner. Authors compared the obtained results, such as compaction and hydraulic conductivity, with those of zeolite. The maximum Proctor densities of two tested zeolites were 1.19 g/cm^3 for Agro Clino Zeolite and 1.34 g/cm^3 for Nat Min 900 zeolite. They also reported that the hydraulic conductivity of Nat Min 900 zeolite was 4.51×10^{-9} m/s at maximum standard Proctor density.

2.2.2 Zeolite – Bentonite Mixtures in Landfill Liner Applications

Kayabalı (1997) investigated some engineering properties of natural zeolite-bentonite mixtures (ZBMs) in order to serve as an impervious liner in sanitary landfills. Regarding the water content and dry density correlations, the author concluded that the obtained results of standard Proctor compaction tests were meaningless. Thus, vibration hammer was used for the compaction. The optimum water content and corresponding dry unit weights were in range of 33-42% and 1.16-1.29 Mg/m^3, respectively. B/Z ratio refers to the dry mass of bentonite to dry mass of zeolite. Also, average hydraulic conductivity of the mixtures which have less than 5% bentonite were obtained in range between $2x10^{-8}$ to $4x10^{-8}$ m/s. Hydraulic conductivity values were generally low at low B/Z ratios. Regarding to its low hydraulic conductivity and high cation exchange capacity, ideal B/Z ratio for landfill liners was reported as 0.05-0.10. Author reported that the use of B/Z mixtures instead of clay liners would significantly reduce the thickness of the base liner for sanitary landfills. Also, it is suggested to use ZBMs as hydraulic barriers and chemical fillers.

Kaya and Durukan (2004) studied on the hydraulic conductivities of ZBMs with different bentonite contents. During the tests, natural zeolites from Bigadiç, (Turkey) were crushed and sieved through #40 sieves and mixed with 3, 5, 10, 20% Na-bentonite. The natural zeolite was non-plastic and liquid limit was 42%. Specific gravity of the zeolite was 2.45, maximum dry unit weight and optimum water content of zeolite was also obtained as 1.31Mg/m^3 and 33%, respectively. The dry unit weights of the mixtures were varied from 1.27 to 1.20 Mg/m^3 while the bentonite content was increased from 3% to 20%. The authors repotted that an increase in the water content caused an increase in the optimum water content and a decrease in the dry unit weight. The hydraulic conductivity tests were performed on the samples with 10 and 20% bentonite contents. The hydraulic conductivities were determined from one-dimensional consolidation apparatus. Hydraulic conductivities of the mixtures were around 1×10^{-9} m/s for all mixtures.

Güney and Koyuncu (2002) investigated the possible use of zeolite as liner material instead of geotextile. For this purpose several laboratory tests were performed in order to determine some engineering properties of ZBM that had 10% bentonite content. The compaction behavior was determined applying standard Proctor compactive effort. Based on compaction test, the optimum water content and maximum dry unit weight of the mixture (B/Z=0.1) were obtained 39% and 16 kN/m^3, respectively. Hydraulic conductivity of the mixtures were determined on samples that were compacted optimum water content. Flexible-wall permeameter were used during hydraulic conductivity tests. The hydraulic conductivity of mixtures were between 1×10^{-8} and 3×10^{-8} cm/sec.

Ören et al. (2011) conducted hydraulic conductivity tests on ZBMs and sand-bentonite mixtures (SBMs). The bentonite contents (BCs) were in the range of 0-30% and 0-20% for ZBMs and SBMs, respectively. Maximum dry unit weights of ZBMs were obtained between 1.04 and 1.12 Mg/m^3 and optimum water contents were between 38% and 45%. However, dry unit weights of SBMs and the optimum water content was less than those of ZBMs. Hydraulic conductivity tests were performed with flexible-wall permeameter. The lowest hydraulic conductivities were obtained when the samples compacted at 2%-5% wet side of the optimum-water content. The hydraulic conductivities of ZBM were between 6.1×10^{-8} and 2.7×10^{-7} cm/s up to 30% bentonite content. The authors reported that the hydraulic conductivity of 10% ZBM was 22 times higher than 10% SBM. Also, the hydraulic conductivity of 20% ZBMs were 28 times higher than that of SBM. It’s also obtained that the grain size effect on the hydraulic conductivity of ZBMs was limited. It’s important to note that the hydraulic conductivity test results were higher than those of previous studies.

Shaquour at al. (2011) studied on two mixtures of volcanic and zeolitic tuffs with marl, sand kaolinite and bentonite in order to determine the best blend which has the highest dry density for using as a low cost landfill liner material. The liquid limit (LL) of the material was 32% and it’s non-plastic. Also, specific gravity is 2.63 Mg/cm^3 for zeolitic tuffs. From the standard Proctor compaction test, maximum dry unit weight of zeolitic tuff was obtained 1.4 g/cm^3. The optimum water content was obtained as 27% for zeolitic tuffs. Authors reported that the maximum dry unit weight and optimum moisture content showed considerable variation depending on the fine content and proportions of the materials in the mixture. If the amount of zeolitic tuff increases, then the maximum dry unit weights decrease and optimum water content increase.

2.4 Application Areas of Zeolite

Due to the following properties natural zeolites have large application areas: (i) cation exchange, (ii) adsorption and related molecular sieving, (iii) catalytic, (iv) dehydration and rehydration, and (v) biological reactivity (Mumpton, 1999). Some popular application areas are given below in detail.

2.4.1 Construction

2.4.1.1 Dimension Stone

Zeolite has been used for 2000 years as a lightweight dimension stone. Because of their low dry unit weights, high porosity, and homogeneous, interconnected texture have make them easily cut into inexpensive blocks (Mumton, 1999). For example, many old towns in central and southern Italy as well as in central Anatolia (Cappadocia) have been built on zeolitic tuff. Moreover, the Greek settlers and Romans, who widely used them, cut as dimension stones and used in constructions (Colella, 2007, chap. 7).

2.4.1.2 Cement and Concrete

Similar with the finely powdered pumice or fly ash, zeolites' high silica content neutralizes excess lime which is produced by setting concrete. This concrete is now known as Roman concrete which is used to build large hydraulic works. For example, Los Angeles aqueduct was constructed, by replacing ≤ 25% of required Portland cement with inexpensive clinoptilolite-rich tuff. (Mumpton, 1999).

2.4.1.3 Lightweight Aggregate

Zeolitic tuffs, which are the excellent aggregates on firing to 1200-1400 ^{0}C from Slovenia and Serbia, can be “popped” by calcining at high temperature. Thus zeolites have been used as lightweight aggregate in concrete. In addition, zeolitic tuffs are used as lightweight insulating material (Mumpton, 1999).

2.4.2 Water and Wastewater Treatment

2.4.2.1 Municipal Wastewater

Clinoptilolites are used in order to extract NH_4^+ from municipal and agricultural waste streams. Clinoptilolites are slow release fertilizers. The negatively charged clinoptilolite structure is held plant nutrients such as nitrogen and potassium and then released on demand. Using clinoptilolite exchanges NH_4^+ from wastewater and provides an ideal growth conditions for nitrifying bacteria at the nitrification sludge, then oxidize NH_4^+ to nitrate (Mumpton, 1999).

2.4.2.2 Drinking Water

Zeolite provides superior performance for sand and carbon filters. It gives purer water and higher output rates with less requirements. Enhance of the clinoptilolite was improved the nitrification of sewage sludge. The clinoptilolite was used for slow-sand filtration of drinking water and reduced the NH_3 content of drinking water from 15-22 down to 2 microns in size. The selectivity of several natural zeolites for Pb^{2+} suggests an inexpensive means of removing lead from drinking water.

2.4.3 Nuclear Waste and Fallout

2.4.3.1 Nuclear Waste

Natural zeolite has a high cation exchange capacity and a particular affinity for heavy metal cations. Zeolite can absorb elements such as strontium 90 (^{90}Sr), cesium 137 (^{137}Cs) and other radioactive isotopes from solutions and hold them in its structure. Clinoptilolite has been used to remove Sr and Cs from low-level effluents before they are released to water from a nuclear power plant (British Nuclear Technology, 1987).

2.4.3.2 Nuclear Fallout

Zeolites are used in radioactive fallout treatments from nuclear tests and accidents. Zeolite apparently exchanges ^{137}Cs and ^{90}Sr in the gastrointestinal treat and is excreted from the body by normal processes. At the Chernobyl fallout, zeolites added to soils in order to reduce the uptake of ^{137}Cs by pasture plants and were prepared for human consumption to counteract.

CHAPTER THREE
MATERIALS AND EXPERIMENTAL METHODS

3.1 Materials

Four different grain sized natural zeolites from two different sources were used in this study. Two of them were obtained from Rota Mining Co. and other two were obtained from İncal Zeolite Co. Both deposits are in Gördes/Manisa that is located in the western part of Turkey.

Zeolites which have less fine content (2-5%) and much sand sized grains (95-98%) were entitled with “granular zeolite” (GZ-1, GZ-2) (Figure 3.1 a-b). Contrarily, zeolites which have more fine content (25-52%) and less sand sized grains (45-61%) were entitled with “fine zeolite” (FZ-1, FZ-2) (Figure 3.1 c-d).

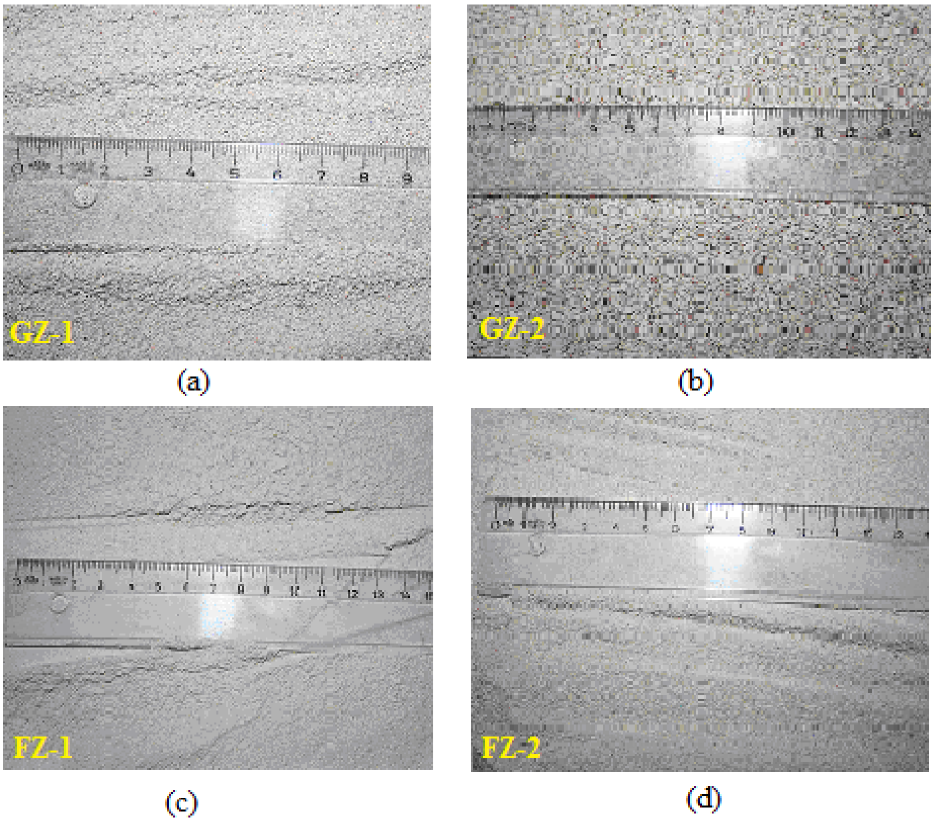

Figure 3.1 Photographic images of tested materials as supplied: a) GZ-1 (granular zeolite from Rota Mining Co.), b) GZ-2 (granular zeolite from İncal Co.), c) FZ-1 (fine zeolite from Rota Mining Co.), d) FZ-2 (fine zeolite from İncal Co.).

Grain size distribution curves of zeolites (granular and fine) are given in Figure 3.2 and corresponding index values are also given in Table 3.1. As depicted in Figure 3.2 and presented in Table 3.1, GZ-1 and GZ-2 are classified as poorly graded sand, SP; FZ-1 is classified as sandy, highly plastic silt, MH; and FZ-2 is also classified as silty sands, SM; according to ASTM D 2487-11 (USCS). The liquid limit and plastic limit are 67.5 and 43.2 for FZ-1 and 59.6 and 45.5 for FZ-2, respectively. Since GZ-1 and GZ-2 have low fine content (i.e.; 2-5%), the consistency limits tests were not performed on these zeolites.

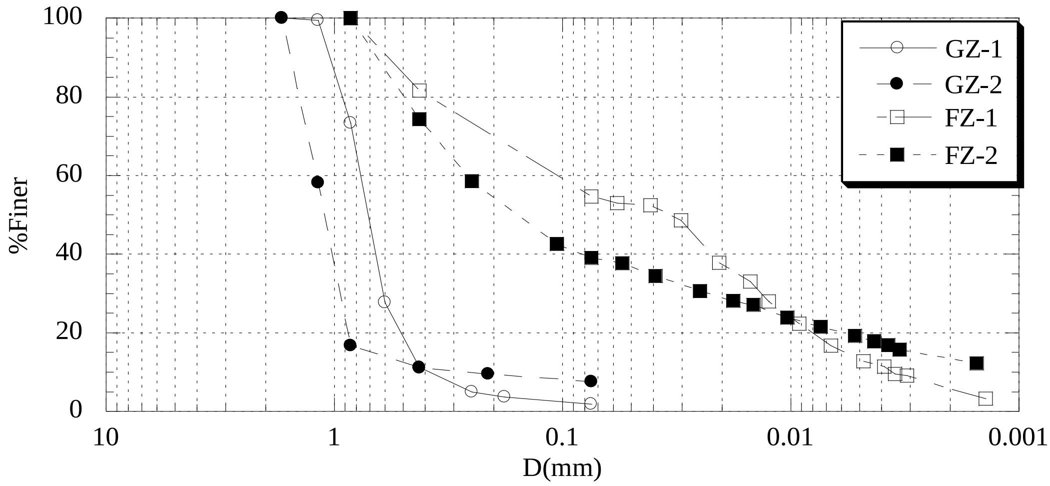

Figure 3.2 Grain size distributions curves of zeolites

Table 3.1 The physical characteristics and index properties of zeolites

	Fine Zeolite		Granular Zeolite		Standards
	FZ-1	FZ-2	GZ-1	GZ-2	
Sand size fraction (%) (2mm - 0.075mm)	45	61*	98	95*	ASTM D 422
Silt size fraction (%) (0.075 - 0.002mm)	52	25*	2	5*	ASTM D 422
Clay size fraction (%) (<0.002mm)	3	14*	-	-	ASTM D 423
Coefficient of Uniformity, C_u	25	200	3.0	6.0	ASTM D2487-11
Coefficient of Curvature, C_c	0.25	2.00	0.75	3.38	ASTM D2487-11
Specific Gravity, G_s	2.34	2.34	2.35	2.35	ASTM D 854-10
Liquid Limit, w_L (%)	67.5	59.6*	-	-	ASTM D 4318-10
Plastic Limit, w_p (%)	43.2	45.5*	-	-	ASTM D 4318-10
Plasticity Index, I_p (%)	24.3	14.1*	-	-	ASTM D 4318-10

*Ören, 2007.

3.2 Experimental Methods

3.2.1 Physical Characteristics and Index Properties

Grain size distributions of zeolites were determined according to the ASTM D 422. Consistency limits were performed on fine zeolites by following ASTM D 4318-10. Specific gravities of zeolites were determined in accordance with ASTM D 854-10.

3.2.2 Compaction Tests

Compaction curves of four different grain sized zeolites were obtained based on ASTM D 698-07. Samples were prepared in their air-dry state and water was added with a spray bottle. The compaction tests were performed after the mixtures prepared. Curing was not applied on wet samples. During the tests 2.5 kg hammer and small mold (10.2 cm diameter and 11.6 cm height) were used. All samples were compacted by applying standard Proctor compaction energy with three layers. After compaction, specimen was removed from the mold using a hydraulic jack.

The optimum moisture content (w_{opt}) and the maximum dry unit weight (γ_{dmax}) for the resulting compaction data were determined by drawing third-order polynomial curve (Howell et al., 1997).

3.2.3 Mini Compaction Tests

Mini compaction test apparatus was manufactured to performed unconfined compression tests. The sample mold has 3.85 cm in diameter and 7.65 cm in height. The hammer was about 1.0 kg and it was designed to fall from a height of 16 cm. Photographic image of mini compaction test apparatus is shown in Figure 3.3. The details of this test apparatus can be followed from Sridharan and Sivapullaiah, 2005.

Figure 3.3 Photographic image of mini compaction apparatus

Prior to unconfined compression tests, mini compaction test apparatus was calibrated. That is, the number of blows need to be determined based on standard Proctor energy. Thus, compaction curves were obtained for mini compaction test by applying 20 and 30 blows per layer. Then, these curves were compared to the referenced compaction curves obtained from standard Proctor compactive effort. As a result, the curves that obtained by applying 20 blows fitted better to the reference curves for FZ-1 and FZ-2. Thus, 20 blows were chosen as an optimal blow count for mini compaction tests.

3.2.4 One-dimensional Consolidation Test

In order to determine the shear rate of zeolites during direct shear test one dimensional consolidation test was performed just on FZ-1. The test was performed according to the ASTM D 2435/D2435M-11. Because it is easy to get saturated, sample was prepared at its liquid limit and then, placed in the oedometer cell 5 kPa seating pressure was applied on the sample. Load increment ratio was set unity and the sample was consolidated under 12.5, 25, 50, 100, 200, 400 and 800 kPa stresses. Each load was maintained until the primary consolidation ended. After the last stress increment was completed, sample was unloaded to 200, 50, 12.5 kPa.

3.2.5 Direct Shear Tests

The shear strength of granular (GZ-1, GZ-2) and fine zeolites (FZ-1, FZ-2) were determined under consolidated-drained (CD) conditions. Samples were prepared at maximum dry unit weight and optimum water content by compacting the zeolite in 6×6 cm square shear box cell.

According to the ASTM D 3080/D3080M-11, direct shear tests were performed under three different normal stresses (0.5, 1.0, 1.5, 2.0 kg/cm^2). The horizontal and vertical displacements and the shear stresses were recorded using transducers with an ADU (Autonomass data acquisition unit) as shown in Figure 3.4.

(a) (b)

Figure 3.4 Photographic images of direct shear apparatus (a) and ADU (b)

Tests were performed after the samples became saturated. For this purpose, GZ-1 and GZ-2 samples were inundated with water for about one hour. On the other hand, FZ-1 and FZ-2 samples were soaked with water for one day in order to get full saturation. Appropriate displacement rates were selected for each sample so that no excess pore pressure would exist at failure. The displacement rate for fine zeolites determined based on the one-dimensional consolidation test results as in the following:

$$t_f = 50\, t_{50} \tag{3.1}$$

$$d_f = d_f / t_f \tag{3.2}$$

where, t_f denotes total estimated elapsed time for failure (min), t_{50} indicates the required time for the specimen achieve 50% consolidation under the specified normal stress (min) and d_f corresponds to the displacement rate (in./mm, mm/min). As a result displacement rates of granular and fine zeolites were 0.1 mm/min and 0.01 mm/min, respectively.

3.2.6 Unconfined Compression Tests

In addition to the direct shear tests, unconfined compressive shear strength was also determined using unconfined compression tests. Since this test is valid only for cohesive soils, GZ-1 and GZ-2 were not tested. Thus only FZ-1 and FZ-2 were subjected to unconfined compression test. The specimens were compacted at maximum dry unit weight and optimum water content using a mini compaction apparatus which was specially designed for unconfined compression tests. Three specimens were tested for each zeolite and the average of these three tests was accepted as the unconfined compression strength. Tests and calculations were carried out as specified in ASTM D 2166-06.

3.2.7 Hydraulic Conductivity Tests

Hydraulic conductivity tests were performed with rigid-wall permeameters at different water contents according to the ASTM D 5856-95 (2007). In order to determine the particle size effect, four different grain sized zeolites were used. Samples were compacted in molds having 10.5 cm diameter and 11.6 cm height by applying Standard Proctor compactive effort. Then, hydraulic conductivity tests were performed. During the hydraulic conductivity tests, tap water was used as the permeant.

Hydraulic conductivity tests were performed by using falling head method for fine zeolites on account of low flow rates. Contrary, hydraulic conductivity of granular zeolites were performed using constant head method due to the rapid flow throughout the sample. During hydraulic conductivity tests, outflow was open to the atmosphere and the water was collected in a graduated cylinder. For both two systems, the average hydraulic gradient was about 20 and the flow was from top to bottom of the specimen. Schematical representations of constant head and falling head type of hydraulic conductivity tests are shown in Figure 3.5a and Figure 3.5b, respectively.

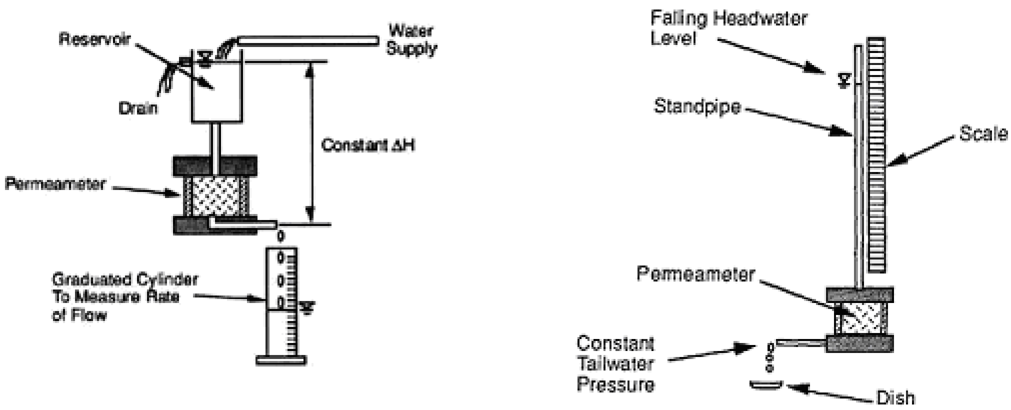

(a) (b)

Figure 3.5 Schematical representations of hydraulic conductivity tests: a) Constant head maintained with overflow drain (Daniel, 1994), b) Falling head test with constant tail-water pressure (Daniel, 1994)

Photographic images of the systems available in our Soil Mechanics Laboratory for constant head method and falling head method are shown in Figure 3.6 and Figure 3.7, respectively.

Figure 3.6 Constant head hydraulic conductivity test set up

Figure 3.7 Falling head hydraulic conductivity test set up

Hydraulic conductivity tests were performed at various water contents: That is, at i) optimum, ii) dry side of optimum, and iii) wet side of the optimum for each zeolite. Test results were expressed in terms of pore volumes of flow (PVF). For example; GZ-1 specimen compacted at optimum water content had about 570 cm^3 voids. This amount of flow corresponds to one pore volume of flow (1 PVF) for the sample. Tests were continued until at least 0.8 PVF and 2 PVF were passed through fine and granular zeolites, respectively. The tests were continued until the hydraulic conductivity values were became constant within the range of ±0.25.

The hydraulic conductivity tests were rapid for compacted granular zeolites than for compacted fine zeolites. The time required for the hydraulic stabilization of fine zeolites was about one day when the samples were compacted at the dry sides of optimum. However, the time required for the hydraulic stabilization of water flow was about 1.5 month when the samples were compacted at optimum and wet side of optimum. To determine the long term hydraulic conductivity behavior of zeolites one test was performed on each FZ-1 and FZ-2.

The hydraulic conductivity for constant head method was calculated based on the equation given below:

$$k = \frac{(Q \times L)}{(\Delta H \times A \times \Delta t)} \tag{3.3}$$

Equation 3.2 was used to calculate hydraulic conductivity for falling head method:

$$k = \frac{(a \times L)}{(A \times \Delta t)} ln\left(\frac{h_1}{h_2}\right) \tag{3.4}$$

In these equations; k is the hydraulic conductivity (cm/s), Q is the flow rate (cm^3), A is perpendicular cross section area through the flow direction (cm^2), a is cross section area of burette (cm^2), L is specimen length (cm), h_1 (cm) and h_2 (cm) are initial and final water level in the burettes, respectively and Δt (s) is the ellapsed time between two readings.

CHAPTER FOUR
TEST RESULTS AND DISCUSSIONS

This chapter presents the test results obtained during this study. In the first part of this chapter, compaction test results are presented. Four different grain sized zeolites (GZ-1, GZ-2, FZ-1, and FZ-2) were subjected to standard Proctor compaction tests and the results are discussed by means of fine content. The compaction tests were also carried out for FZ-1 and FZ-2 using a special designed mini compaction test apparatus. The results are compared to those of standard Proctor compaction.

In order to obtain the shear rate of zeolites, one-dimensional consolidation test was performed on FZ-1. The results of this test are presented in the second part.

In the third part of this chapter, shear strength results of zeolites are presented. For this purpose, consolidated drained shear strength properties of zeolites were determined from direct shear tests. Also, unconfined compressive strength properties of FZ-1 and FZ-2 were determined.

Finally, hydraulic conductivity characteristics of zeolites are given in terms of compaction water contents.

4.1 Compaction Test Results

4.1.1 Standard Proctor Compaction Tests Results

Compaction characteristics of zeolites were investigated based on different grain size. Compaction characteristics of a material are expressed with maximum dry unit weight and optimum water content. The compaction tests were performed only with standard Proctor compaction effort at various water contents. Although it was difficult to compact granular zeolites, bell-shaped compaction curves were obtained for four zeolites. The compaction curves of GZ-1, GZ-2, FZ-1 and FZ-2 are shown in Figure 4.1. The compaction parameters (i.e. maximum dry unit weight and optimum water content) obtained from these curves are summarized in Table 4.1.

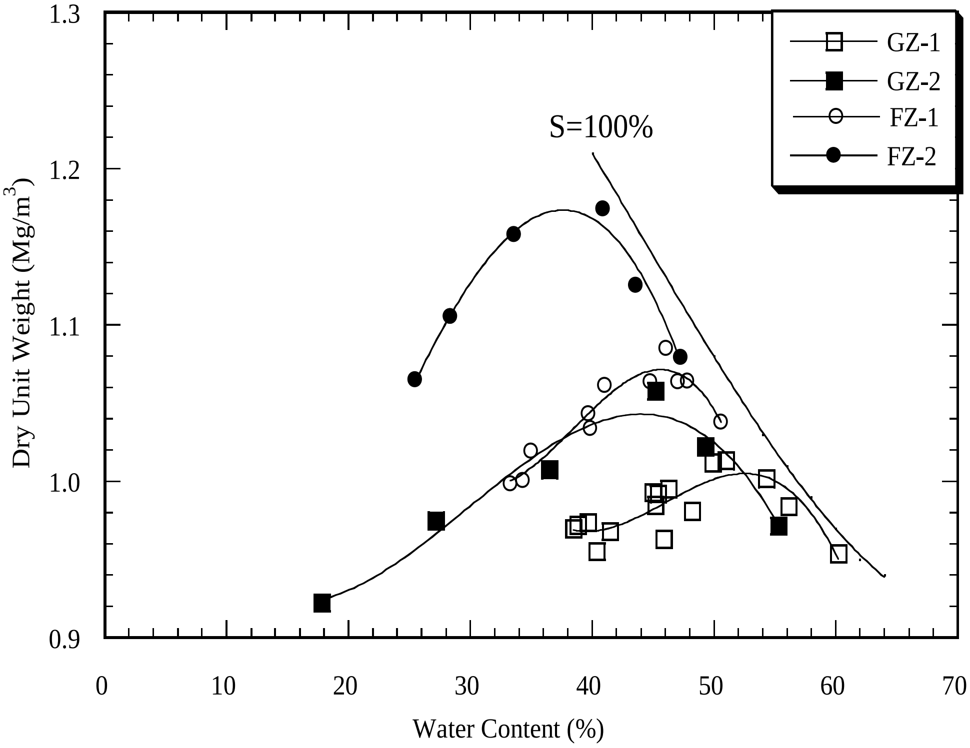

Figure 4.1 Compaction curves of GZ-1, GZ-2, FZ-1 and FZ-2

Table 4.1 Standard Proctor compaction parameters of GZ-1, GZ-2, FZ-1 and FZ-2

Sample	ρ_{dmax} (Mg/m^3)	w_{opt} (%)
GZ-1	1.01	52
GZ-2	1.04	44
FZ-1	1.07	47
FZ-2	1.17	38

As seen in Figure 4.1 and Table 4.1, maximum dry unit weights (ρ_{dmax}) of zeolites were between 1.01 and 1.17 Mg/m^3 and optimum water contents were between 38% and 53%. Figure 4.1 shows that increasing the grain size lead to decrease the maximum dry unit weights. In other words, increase in the amount of fine contents lead to increase maximum dry unit weights. Regardless of grain size, maximum dry unit weight values of zeolites were significantly less than that of sands and clays. For example, dry unit weight values change between 1.5 and 2.3 Mg/m^3 for sands and gravels, 0.6 and 1.8 Mg/m^3 for silts and clays (Holtz, Kovacs & Sheahan, 2011).

Low dry unit weights for zeolites are possibly because of highly porous structure of zeolites. Although GZ-1 and GZ-2 have similar particle size with sands, zeolites are compacted better than sands. Since capillarity forces are small for sands on account of large pores, the conventional compaction curves can not be obtained for sands. However, the structure of zeolites consists of thin channels. This may lead high capillarity forces than sand. In addition, 2-5% fine content GZ-1 and GZ-2 enable zeolites to be compacted better than sands.

There is scarce data related to compaction behavior of zeolites in the literature. Regarding to maximum dry unit weight and optimum water content, only six data were found from the literature (Navia et al., 2005; Shaquor et al., 2011; Yuan, 1997). The findings of this study and those of literature are evaluated together as a function of fine content (Figure 4.2). Figure 4.2 indicates that maximum dry unit weight increased and optimum water content decreased up to 30% fine content. Above 30% fine content, maximum dry unit weight decreased and optimum water content increased as the fine content further increased. The data reported by Navia et. al.

(2005) are close to the findings in this study. This may be attributed to the use of same type of zeolites (clinoptilolite) in this study and the study of Navia et. al. (2005). It should be noted that the specific gravities of clinoptilolites which were used in two studies are closed within each other (i.e. 2.34 for this study and 2.2 for Navia et. al., 2005). The data of Shaquor et. al (2011) and one data from Yuan (1997) (clinoptilolite was referred as CLN) have higher maximum dry unit weights and lower optimum water contents than the findings of this study. Although the data from Yuan (1997) is clinoptilolite type of zeolite, specific gravities of zeolites in both Shaquor et. al. (2011) and Yuan (1997) are higher than the specific gravities of zeolites in this study. Also, one data from Yuan (1997) (chabazite was named as CHB) has lower dry unit weights and higher optimum water contents than those of data in this study. Although specific gravities of zeolites used in this study and CHB used in Yuan's study are almost the same (2.34 for this study, 2.32 for CHB), the differences between the compaction parameters may be due to the structural diversity of chabazite and clinoptilolite.

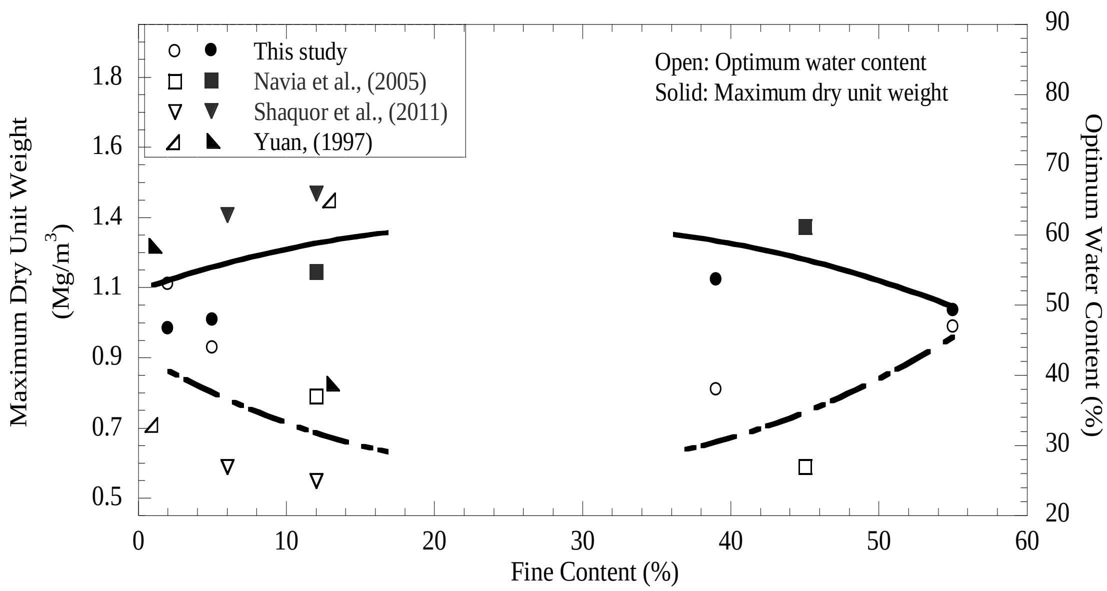

Figure 4.2 Maximum dry unit weight variation with fine content

4.1.2 Mini Compaction Test Results

To determine equivalent blow number for mini compaction test with respect to standard Proctor compaction, two compaction tests, one with 20 blows and the other with 30 blows per layer, were conducted on FZ-1 and FZ-2. The compaction curves obtained from mini compaction tests are shown in Figure 4.2 together with standard Proctor compaction curves. Standard Proctor compaction curves are named with "reference curves" when compared to mini compaction test curves.

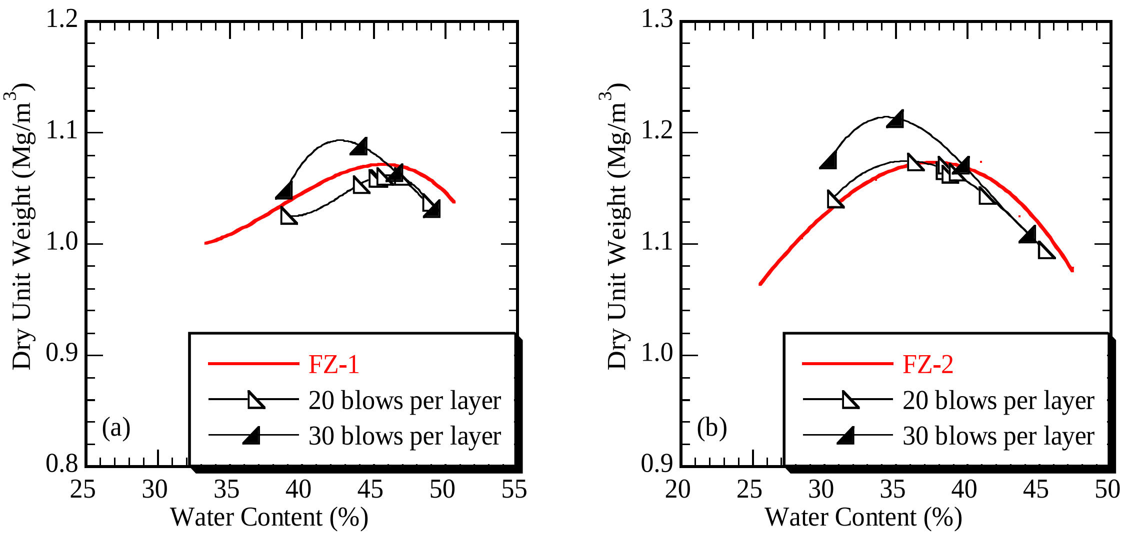

Figure 4.3 Compaction curves obtained from mini compaction tests for: a) FZ-1, b) FZ-1

The curves that were obtained with 20 blows per layer for both FZ-1 and FZ-2 fit better to the reference curves. As a result, 20 blows per layer were chosen as optimal blow number to prepare samples for unconfined compression tests.

4.2 Consolidation Test Results

Figure 4.4 shows the compressibility behavior of FZ-1 as a function of effective stress. Compression index (C_c) of FZ-1 is calculated with the following equation:

$$C_c = \frac{\Delta e}{\Delta log\sigma'} \tag{4.1}$$

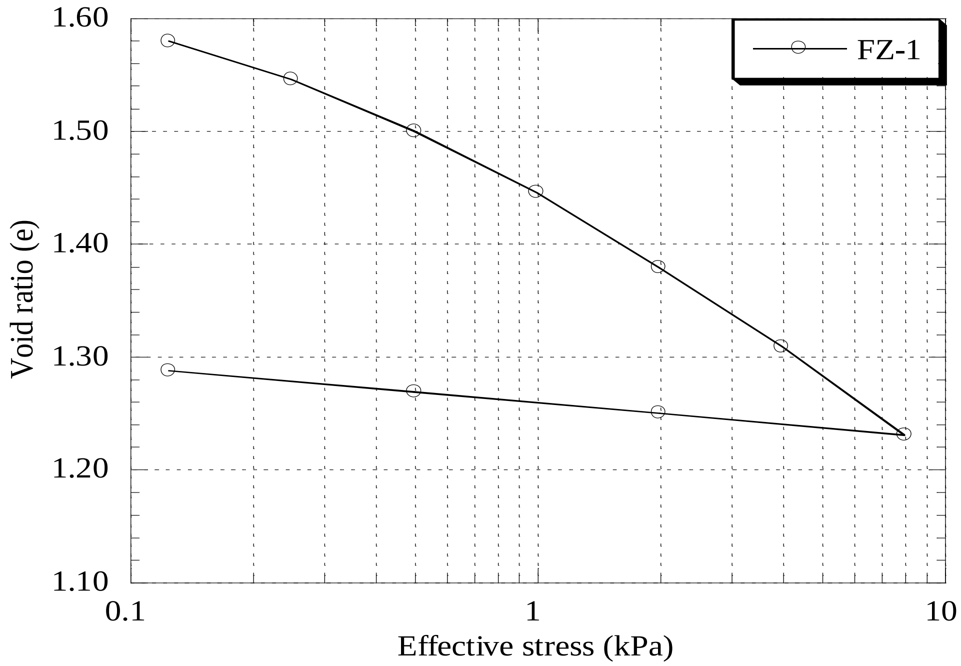

Figure 4.4 Void ratio (e) – log pressure diagram of FZ-1

Compression index (C_c) is obtained as 0.237 from Figure 4.4. Also, coefficient of consolidation (c_v) for FZ-1 was determined with Taylor's square root of time fitting method. In this method, dial readings were plotted versus square root time in linear scale. Then, t_{90} values were determined. Coefficient of consolidation (c_v) parameters are determined with the following equation. Relevant consolidation diagrams for each loading levels are given in Figure 4.5.

$$c_v = \frac{0.848 \times {H_{dr}}^2}{t_{90}} \tag{4.2}$$

where, H_{dr} expresses the drainage path length during the oedometer tests, t_{90} denotes the required time for the 90% of consolidation completed.

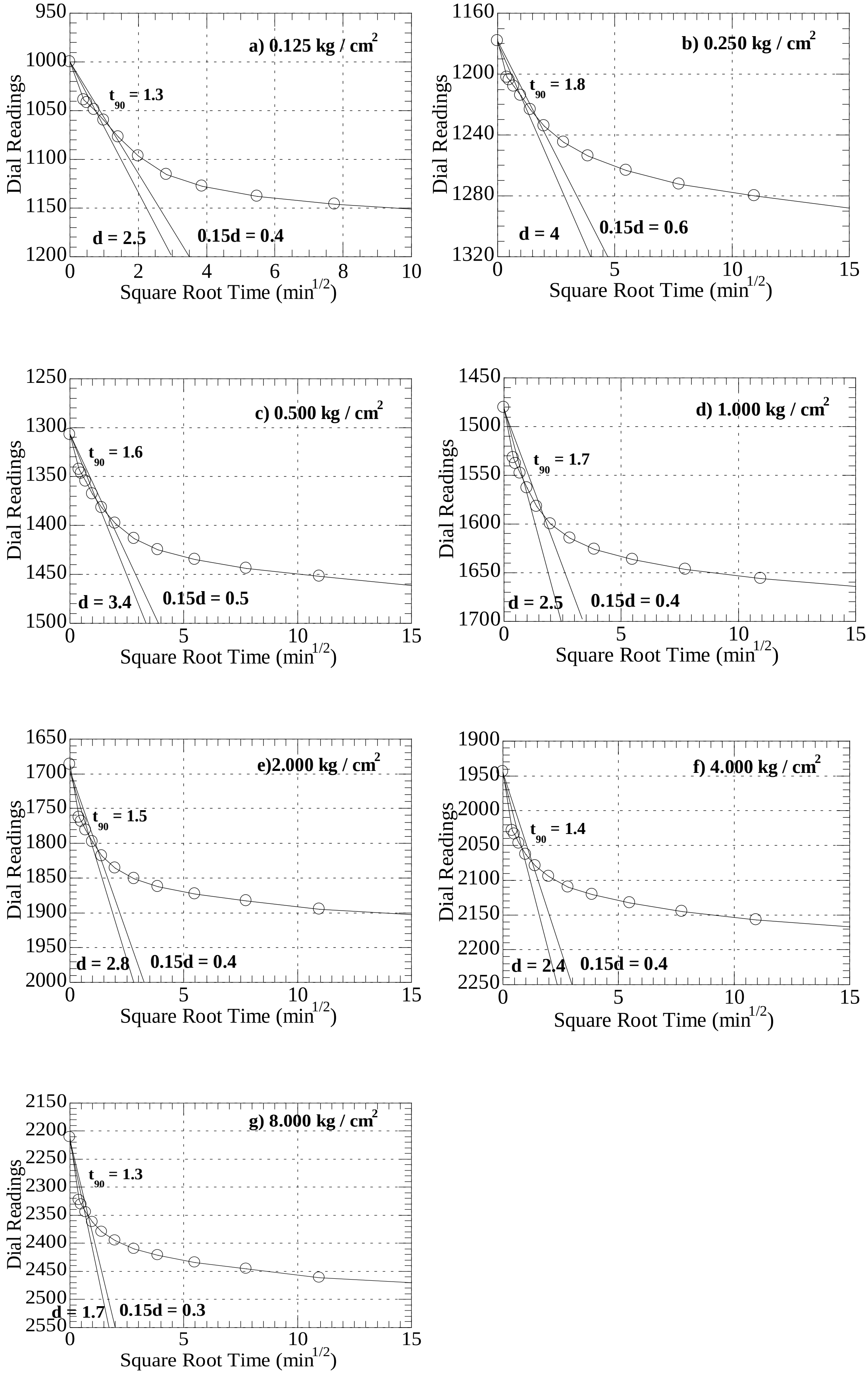

Figure 4.5 Dial readings versus square root time

The average coefficient of consolidation (c_v) parameter was obtained from Figure 4.5 as 0.335 cm^2/min.

Similarly, Yükselen-Aksoy (2010) performed consolidation tests on two different zeolites. One of which has 12% and the other has 1% sand sized particles. Both zeolites were tested at their liquid limits. The reported compression index values were 0.194 and 0.130, which is less than that of FZ-1 in this study. She also reported the values of coefficient of consolidation parameters as 0.02 cm^2/min for Z-1 and 0.077 cm^2/min for Z-2 which is about fifteen times less than that of FZ-1. It is possibly because of larger fine content of zeolites used in her study (i.e. 88% for Z-1 and 99% for Z-2).

4.3 Direct Shear Test Results

The stress-strain curves obtained from direct shear tests for each zeolite are shown in Figure 4.6. Figure 4.6 illustrates the variation of shear stress versus axial strain. For every normal force level, maximum shear stress value is regarded as peak shear strength of the soil. Peak shear strength values with respect to loading levels for each zeolite are given in Table 4.2.

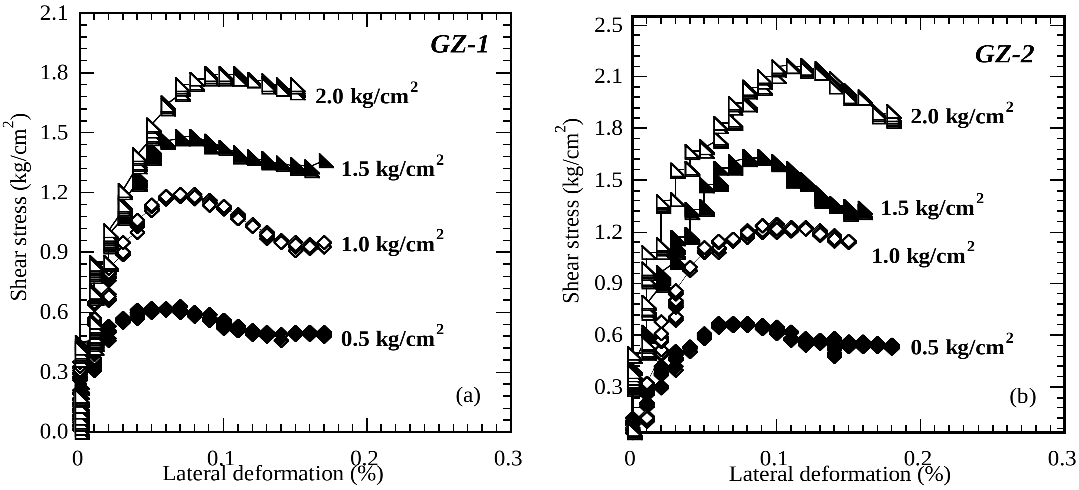

Figure 4.6 Stress-strain curves: a) GZ-1, b) GZ-2, c) FZ-1, d) FZ-2

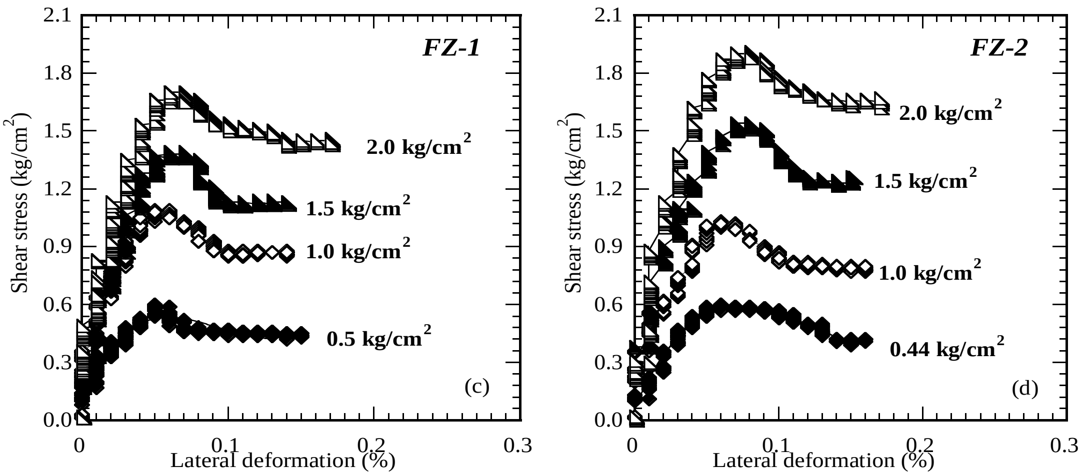

Figure 4.6 continued.

Table 4.2 Direct shear test results

GZ-1		GZ-2		FZ-1		FZ-2	
σ_f ' (kg/cm^2)	τ_f ' (kg/cm^2)	σ_f ' (kg/cm^2)	τ_f ' (kg/cm^2)	σ_f ' (kg/cm^2)	τ_f ' (kg/cm^2)	σ_f ' (kg/cm^2)	τ_f ' (kg/cm^2)
0.5	0.630	0.5	0.670	0.5	0.602	0.44	0.602
1.0	1.200	1.0	1.265	1.0	1.087	1.0	1.030
1.5	1.487	1.5	1.670	1.5	1.394	1.5	1.544
2.0	1.940	2.0	2.227	2.0	1.709	2.0	1.907

As seen from Figures 4.6 a-d and Table 4.2, the peak shear strength of all zeolites increases when the effective normal stress increases. In order to determine the internal friction angel and cohesion intercept for each zeolite shear strengths versus effective normal stresses at failure are plotted. Mohr failure envelopes of each zeolite are given in Figure 4.7.

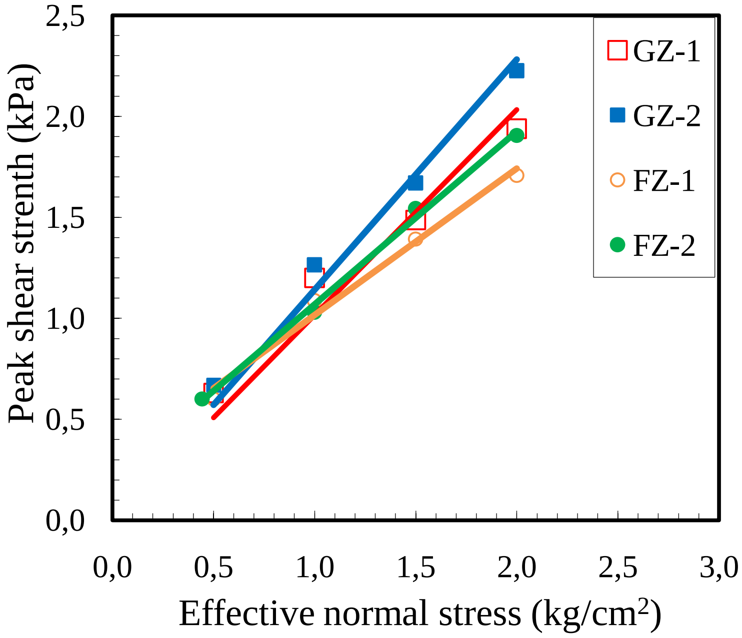

Figure 4.7 Mohr failure envelopes of GZ-1, GZ-2, FZ-1 and FZ-2

According to the obtained failure envelopes, GZ-1 and GZ-2 have almost no cohesion intercepts. However, the cohesion intercepts of FZ-1 and FZ-2 were determined as 0.291 kg/cm^2 and 0.211 kg/cm^2, respectively. Also, the drained internal friction angles are 45.5°, 48.8°, 36° and 40.6° for GZ-1, GZ-2, FZ-1 and FZ-2, respectively. Also the relationship between internal friction angles and fine contents of zeolites are given in Figure 4.8.

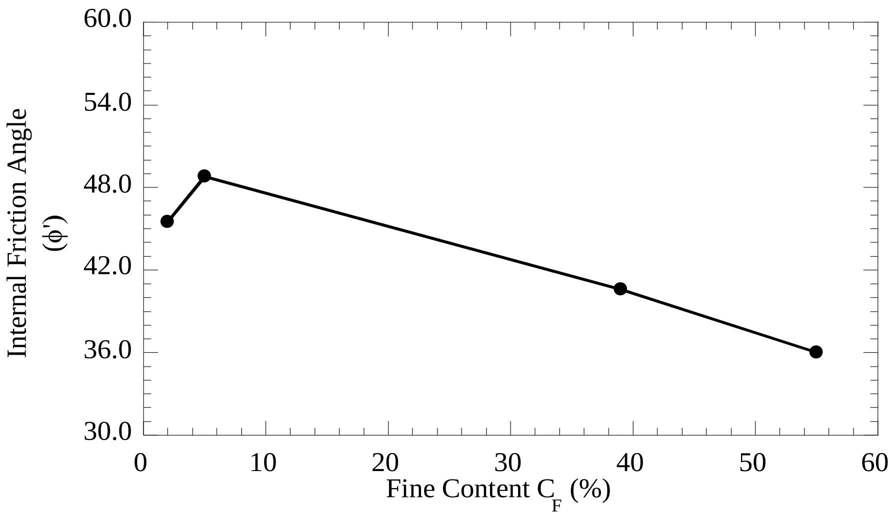

Figure 4.8 Relationship between internal friction angle and fine content of zeolites

In this study consisting of 5% fine content zeolite resulted the highest internal friction angle. Above the 5% fine content internal friction angles of zeolites decreased.

Although there is no comprehensive study on shear strength parameters of zeolites, Yükselen-Aksoy (2010) reported the direct shear tests of two different zeolites (Z-1 and Z-2) which were classified as ML and MH. In this study, it was reported that the cohesion intercepts for both two zeolites were equal to zero and internal friction angels were obtained as 34° and 36.5°, respectively. Because FZ-1 is classified as MH, the reported values are close to the reported results. The internal friction angles of GZ-1, GZ-2 and FZ-2 are higher than those of Z-1 and Z-2.

Since GZ-1, GZ-2 and FZ-2 were classified as SP and SM, their shear strength parameters could be compared with sands. The internal friction angles of dense sands are in the range between 35° and 47° (Holtz, Kovacs & Sheahan, 2011). Thus, it's concluded that the mechanical properties of compacted zeolites are almost the same with dense sands.

4.4 Unconfined Compression Test Results

Unconfined compressive strength values of FZ-1 and FZ-2 are given in Table 4.3. Stress conditions in the unconfined compression tests are similar with unconsolidated undrained (UU) tests. The only difference between these two tests is the cell pressure (or confining pressure) equals to zero in unconfined compression tests. Thus, effective stress conditions at failure are the same with UU tests and practically shear strength parameters obtained from unconfined compressive tests are identical with undrained shear strength parameters. For FZ-1 and FZ-2, unconfined compressive strength versus deformation behavior is given in Figure 4.9.

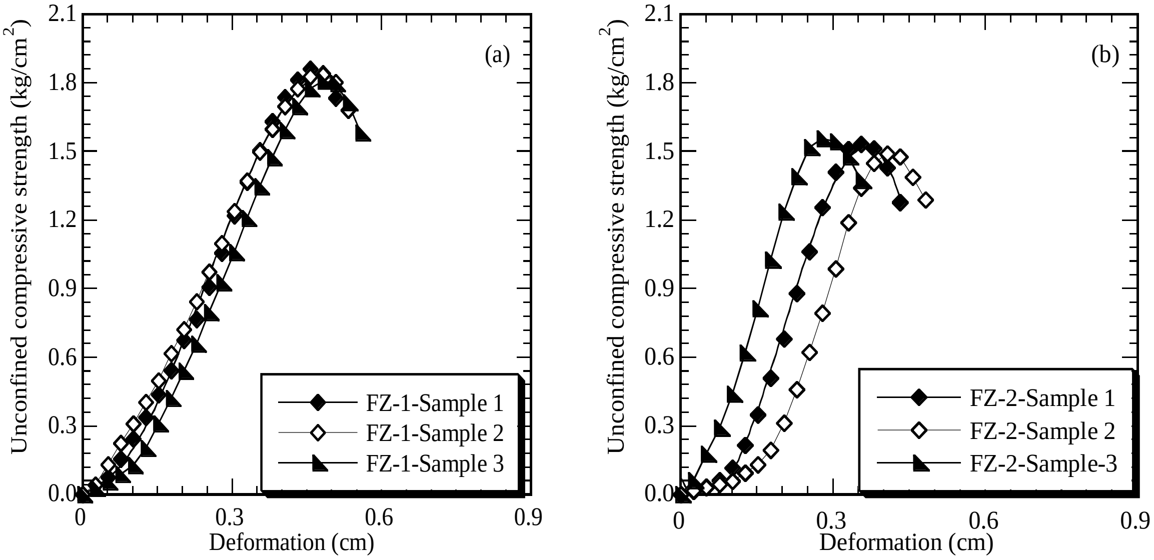

Figure 4.9 Unconfined compressive strength of a) FZ-1, b) FZ-2

The average unconfined compressive strength values of FZ-1 and FZ-2 are 1.83 kg/cm^2 and 1.52 kg/cm^2, respectively. As seen in Figure 4.9 FZ-1 has higher unconfined compressive strength than FZ-2. The reason for this may be attributed to the higher fine content of FZ-1 than FZ-2.

Table 4.3 The properties of unconfined compression test samples

FZ-1			FZ-2		
Water content %	γ_{dmax} (Mg/m^3)	Unconfined compressive strength (kg/cm^2)	Water content %	γ_{dmax} (Mg/m^3)	Unconfined compressive strength (kg/cm^2)
45.07	1.06	1.83	38.18	1.17	1.53
45.18	1.06	1.86	38.28	1.17	1.49
45.61	1.06	1.81	38.59	1.16	1.56

4.5 Hydraulic Conductivity Test Results

The hydraulic conductivity tests were carried out at various water contents. The locations of the test points were placed on the compaction curves as shown in Figure 4.10.

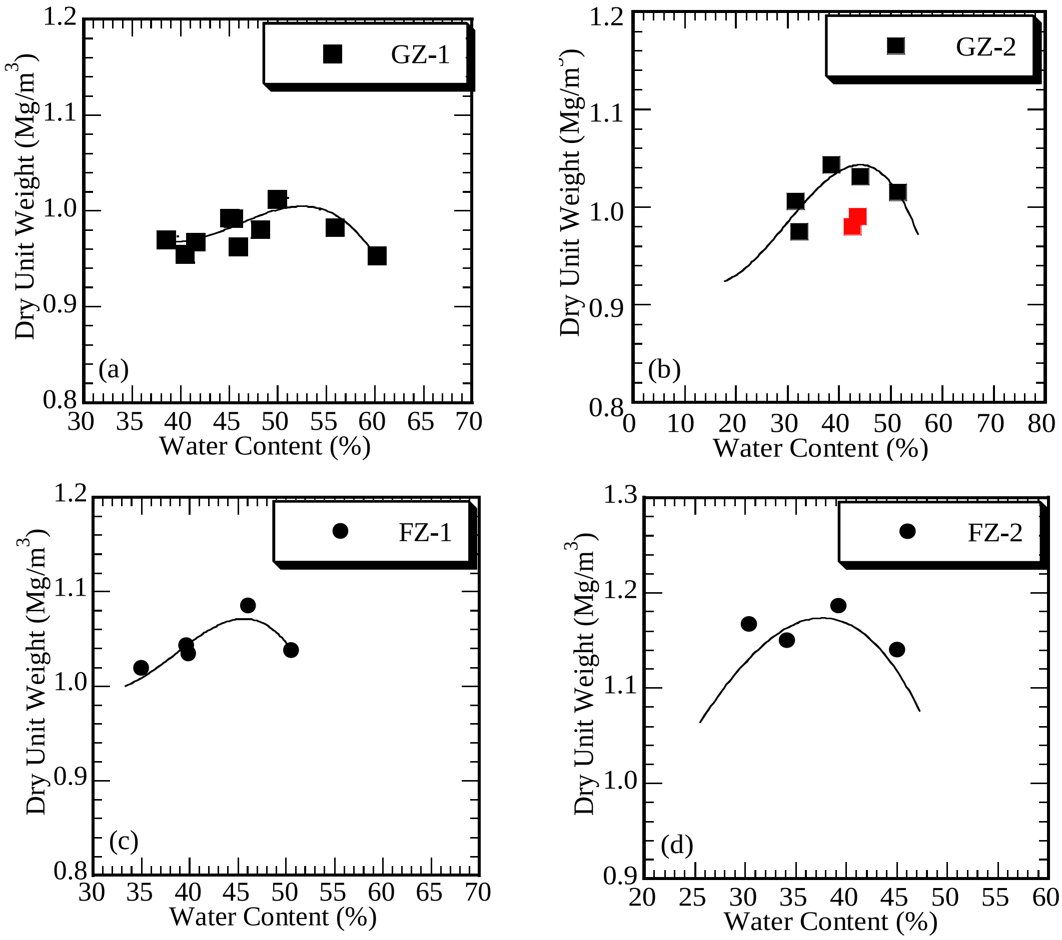

Figure 4.10 Locations of the hydraulic conductivity test samples on compaction curves: a) GZ-1, b) GZ-2, c) FZ-1 and d) FZ-2

As seen in Figure 4.10, except two samples for GZ-2, all hydraulic conductivity samples meet well with predetermined compaction curves. The two samples tested for GZ-2 were at optimum water content, but far below their targeted dry unit weight (represented with red solid squares). Also, values of compaction parameters of hydraulic conductivity samples are summarized in Table 4.4.

Table 4.4 Compaction parameters of hydraulic conductivity test samples

FZ-1		FZ-2		GZ-1		GZ-2	
w%	γ_d	w%	γ_d	w%	γ_d	w%	γ_d
35.0	1.02	30.4	1.17	38.5	0.97	31.6	1.01
39.7	1.04	34.2	1.15	40.4	0.95	32.3	0.98
39.9	1.03	39.3	1.19	41.5	0.97	38.5	1.04
46.1	1.08	45.2	1.14	45.0	0.99	42.6*	0.98
50.64	1.04			45.5	0.99	43.6*	0.99
				45.9	0.96	44.1	1.03
				48.2	0.98	51.4	1.01
				49.9	1.01		
				55.9	0.98		
				60.2	0.95		

*Far from the standard Proctor compaction curve (represented with red squares)

4.5.1 Constant Head Hydraulic Conductivity Test Results

The hydraulic conductivity of compacted granular zeolites at various water contents are shown in terms of pore volumes of flow (PVF). Hydraulic conductivity test results for GZ-1 are represented in Figure 4.11 a-i. Also hydraulic conductivity test results of GZ-2 are shown in Figure 4.13 a-g.

Most of the hydraulic conductivity tests on GZ-1 were terminated within a day. In some cases, the hydraulic stability was not achieved at the end of the day. Then, the inflow valve was closed. The tests were begun in the next morning again. This procedure was repeated until the four hydraulic conductivity readings were within the range of ± 25%. The results of this experiment are shown in Figure 4.11 a, b, f, g, and h. As seen in the figures, hydraulic conductivities of some specimens decreased during the day and valves were closed at the end of the day. Samples lost their water contents until the tests were started again. Thus, the hydraulic conductivity of the specimen became higher than the last readings.

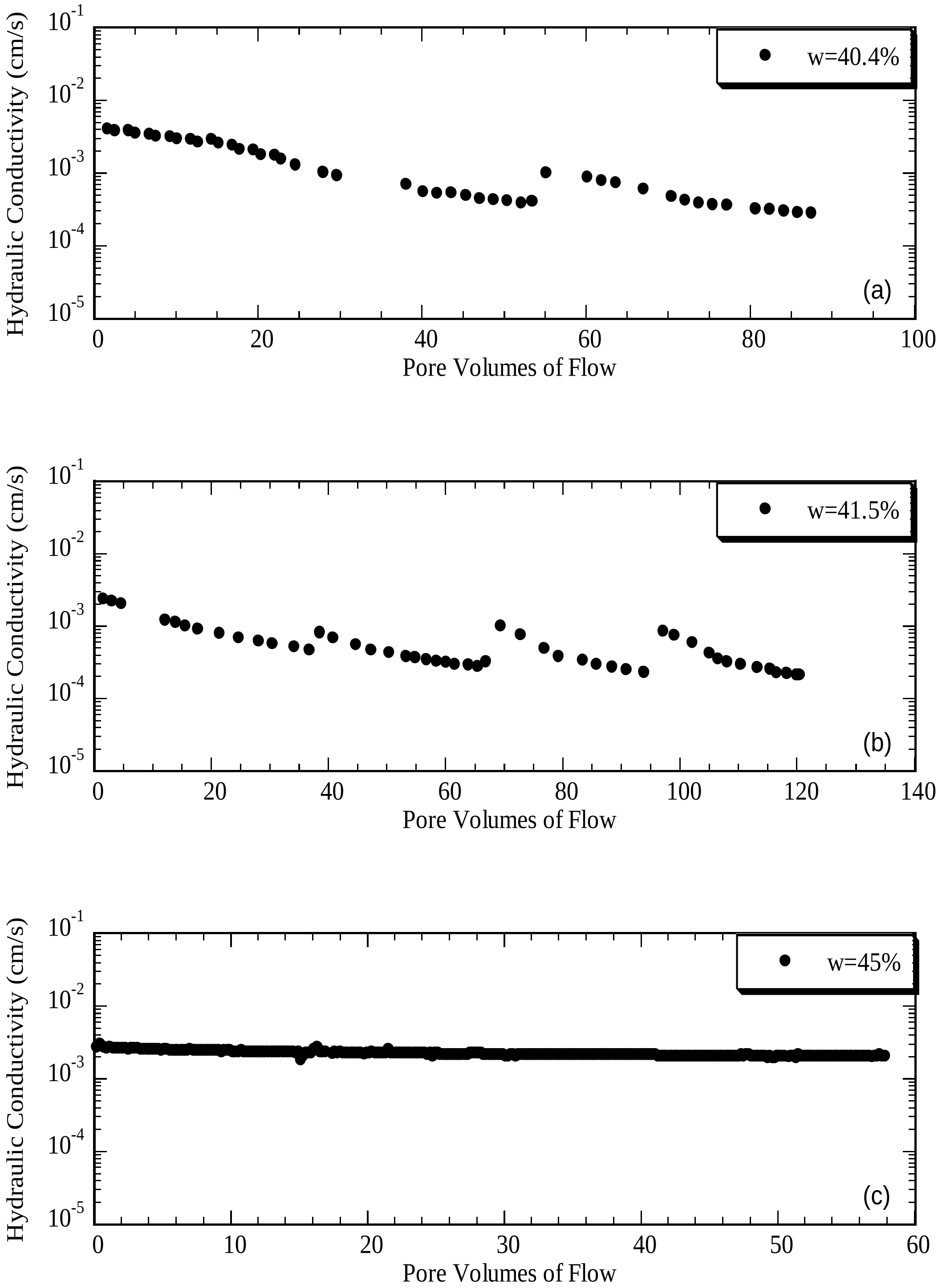

Figure 4.11 Hydraulic conductivity test results of GZ-1

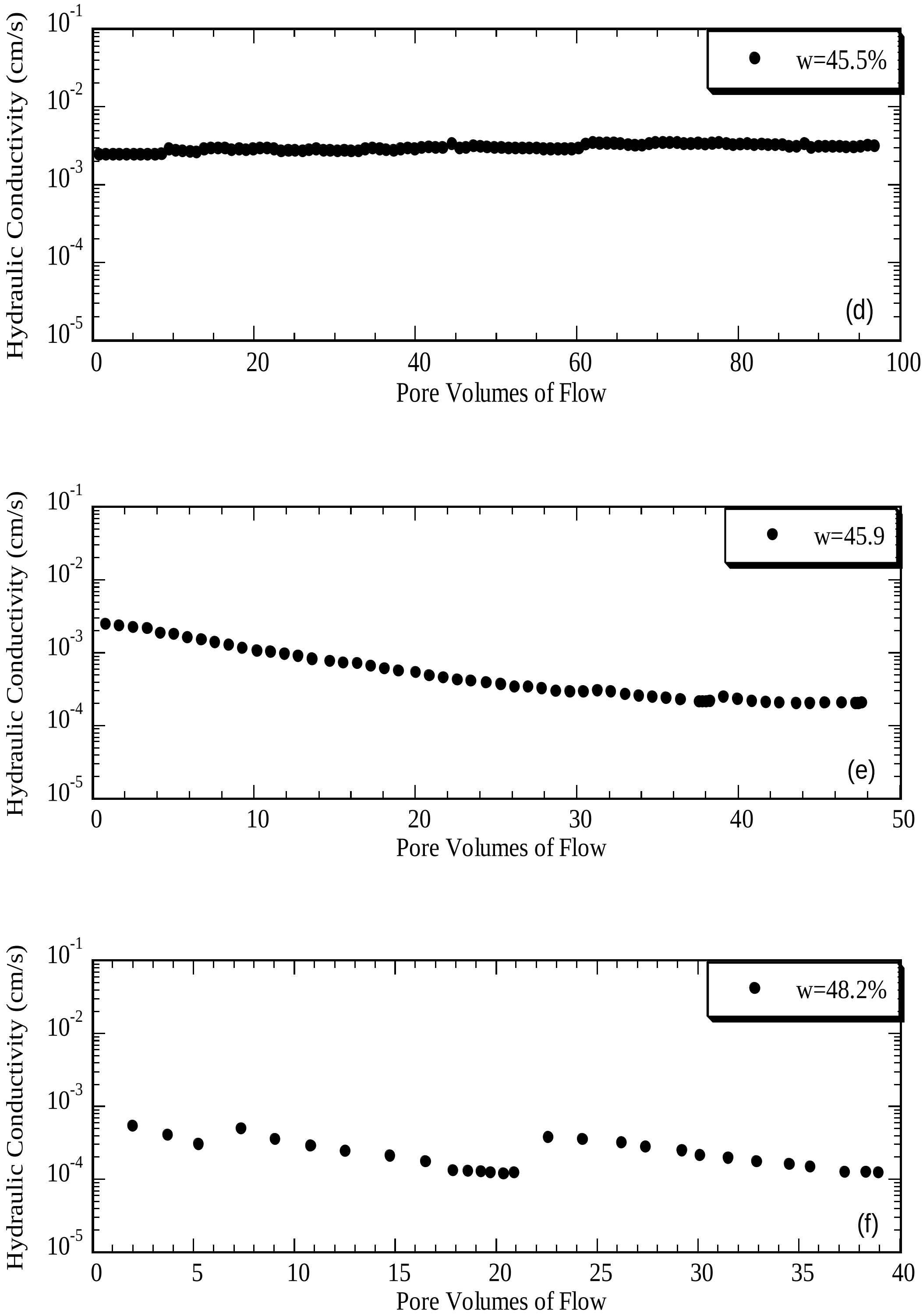

Figure 4.11 continued.

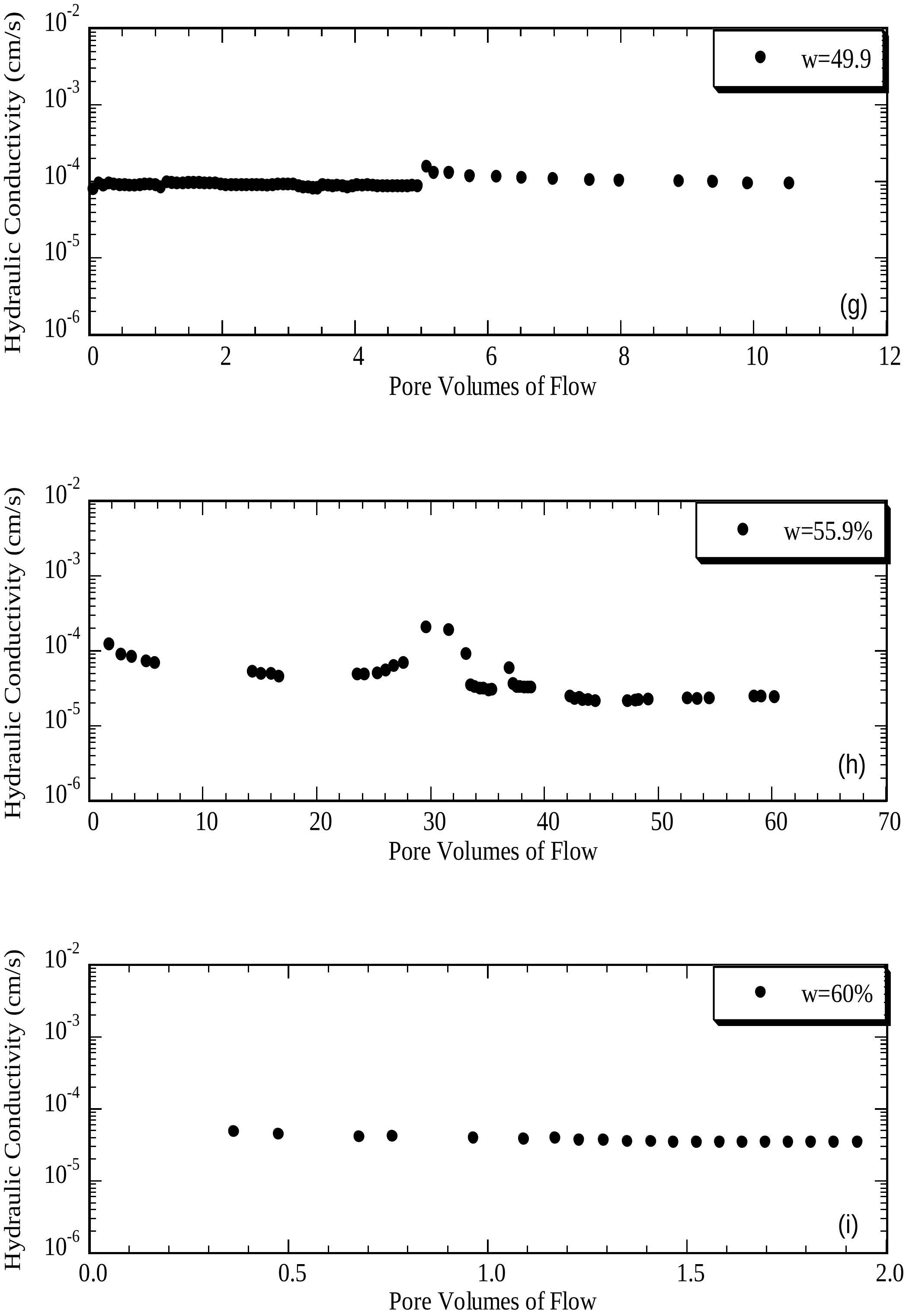

Figure 4.11 continued.

As seen in Figure 4.11 a-i, at the dry side of the optimum water content hydraulic conductivity values of GZ-1 decreased about one order of magnitude at the end of the test. However, at the optimum water content and the wet side of the optimum water content, this reduction was observed less than that of observed at the dry side of the optimum water content.

Generally, an increase in the compaction water content led to a decrease in the hydraulic conductivity. Thus, the representation of all hydraulic conductivity test results for GZ-1 is divided into two groups. Figure 4.12a shows the results of the samples that had water content less than optimum and Figure 4.12b shows the hydraulic conductivity results of the samples that had water contents at or higher then optimum.

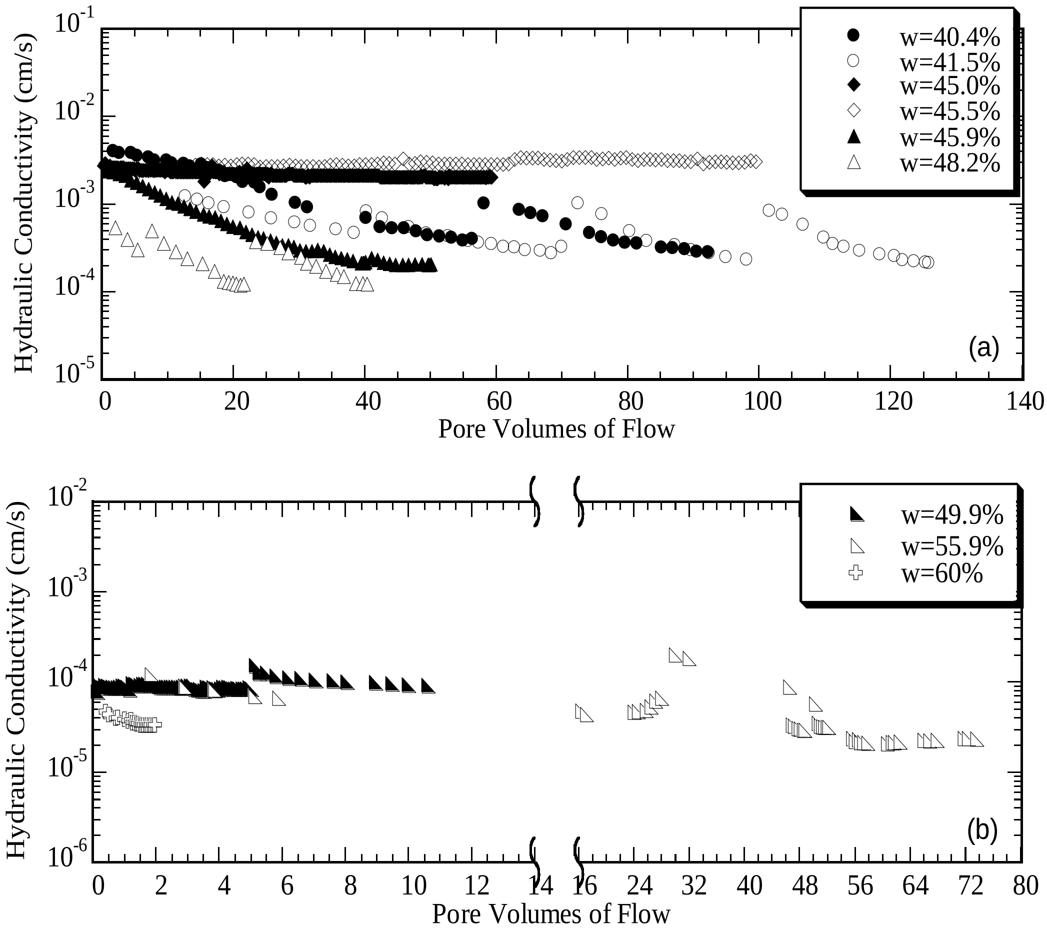

Figure 4.12 Hydraulic conductivity behavior of GZ-1: a) Results for samples $w < w_{opt}$, b) Results for samples $w \geq w_{opt}$

As seen in Figure 4.12a and Figure 4.12b, hydraulic conductivity values of GZ-1 decreased about two orders of magnitude when the compaction water content was increased. Table 4.5 summarizes the final hydraulic conductivity test results of GZ-1.

Table 4.5 Hydraulic conductivity of GZ-1 at various water contents

Sample No	w %	γ_d	k_{final} (cm /s)
1	38.5	0.97	5.16×10^{-3}
2	40.4	0.95	2.83×10^{-4}
3	41.5	0.97	2.12×10^{-4}
4	45.0	0.99	2.02×10^{-3}
5	45.5	0.99	3.07×10^{-3}
6	45.9	0.96	2.04×10^{-4}
7	48.2	0.98	1.21×10^{-4}
8	49.9	1.01	9.33×10^{-5}
9	55.9	0.98	2.41×10^{-5}
10	60.2	0.95	3.44×10^{-5}

Similarly, hydraulic conductivity test results for GZ-2 are shown in Figure 4.13a-g in terms of PVFs.

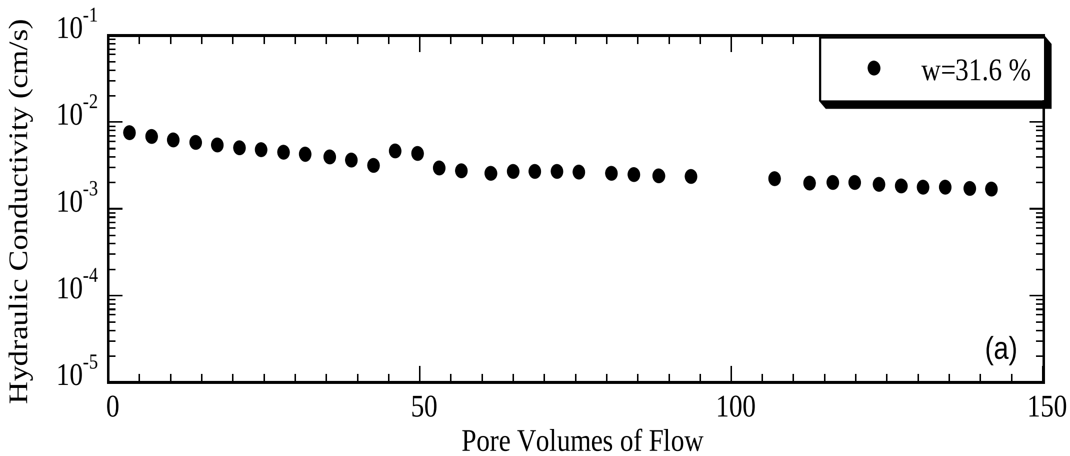

Figure 4.13 Hydraulic conductivity test results of GZ-2

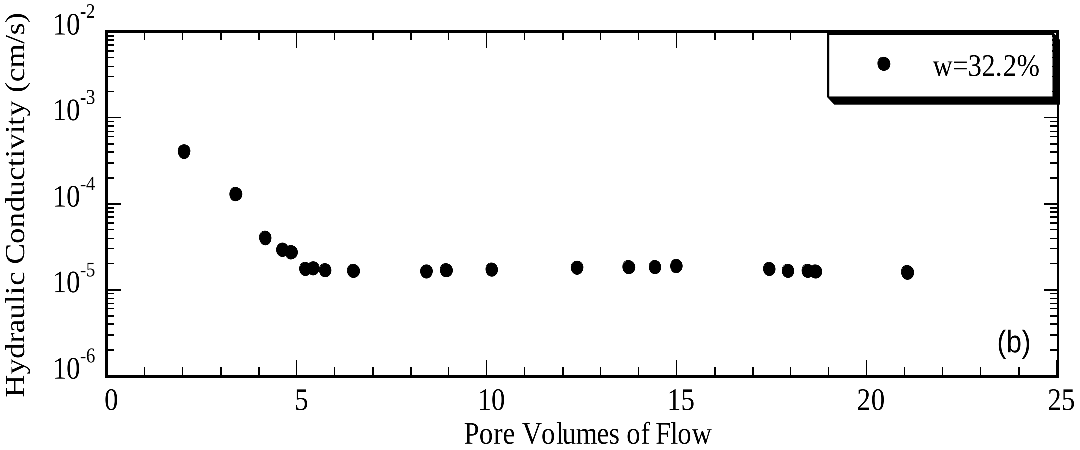

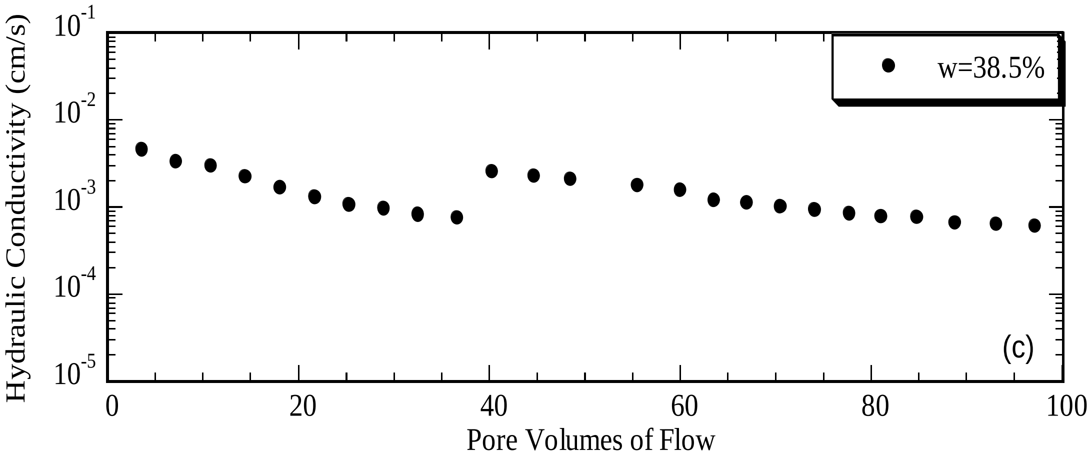

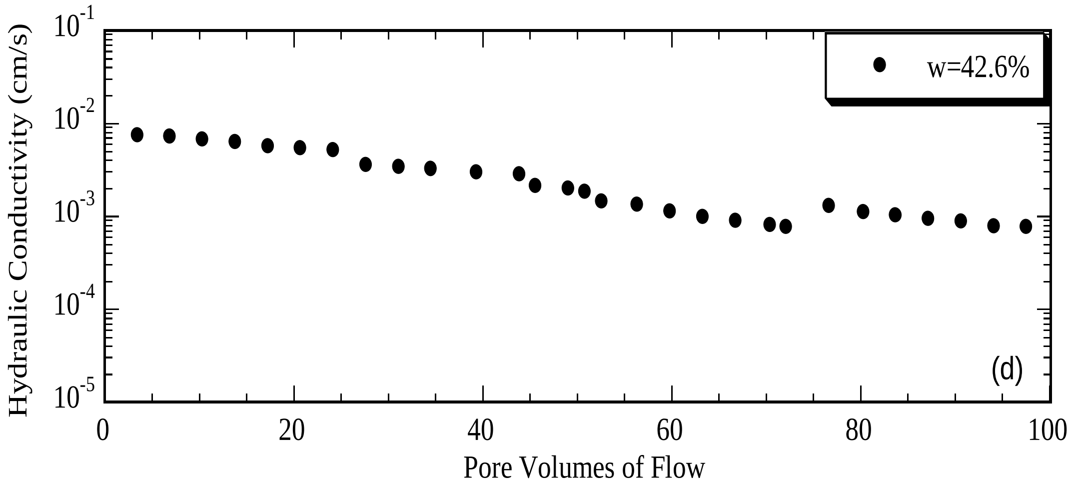

Figure 4.13 continued.

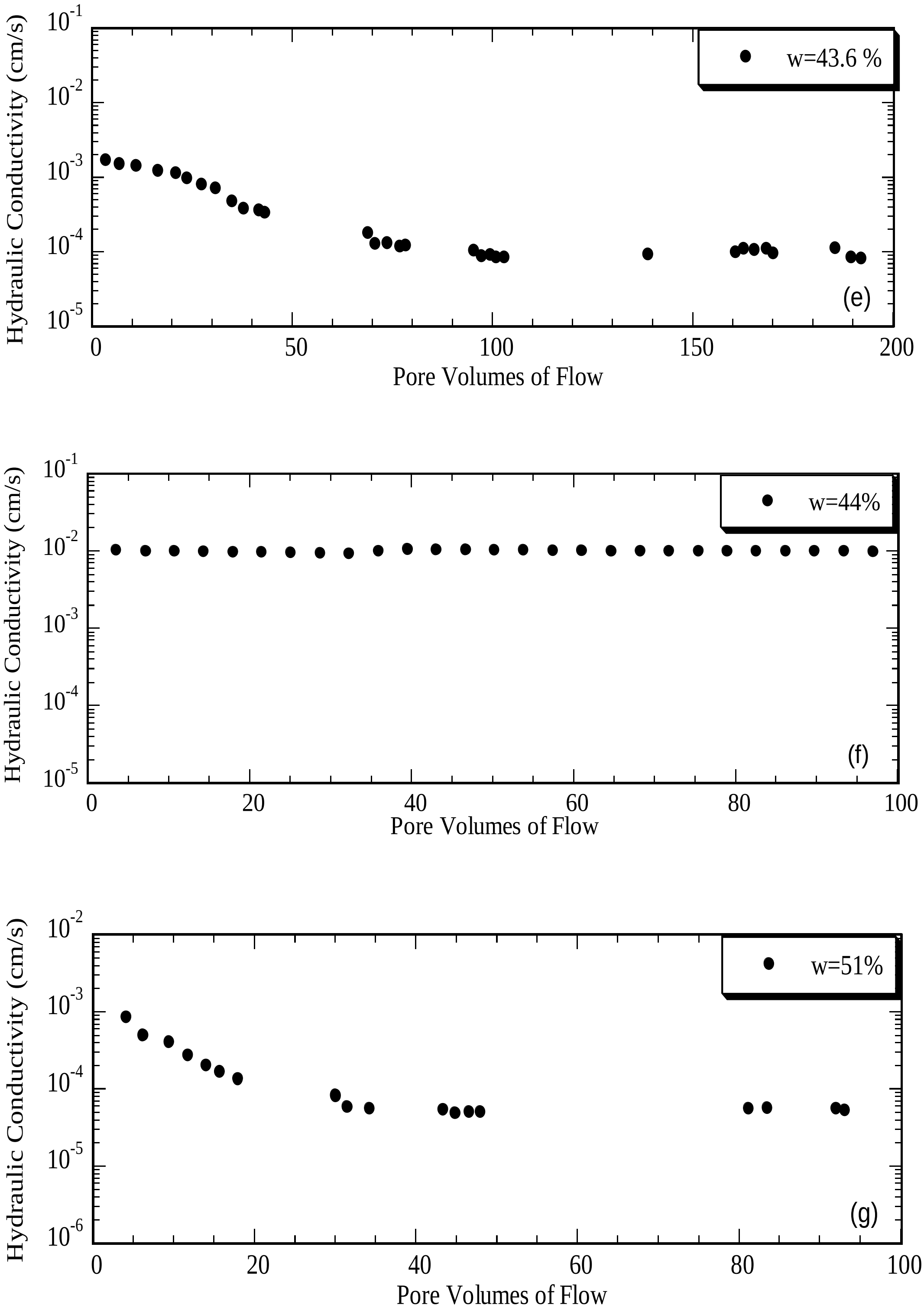

Figure 4.13 continued.

As seen in the Figure 4.13 a-e, until the optimum water content, hydraulic conductivity values decreased maximum 25 times from the initial values. Hydraulic conductivity values almost unchanged during the test when the compaction water content was at optimum. However, at the wet side of the optimum water content initial hydraulic conductivity values decreased 16 times until the desired termination criteria was achieved.

Hydraulic conductivity tests for GZ-2 were performed until minimum 22 PVFs and maximum 150 PVFs passed through the samples. Representation of the all hydraulic conductivity test results of GZ-2 is shown in Figure 4.14. Also, final hydraulic conductivity test results are summarized in Table 4.6.

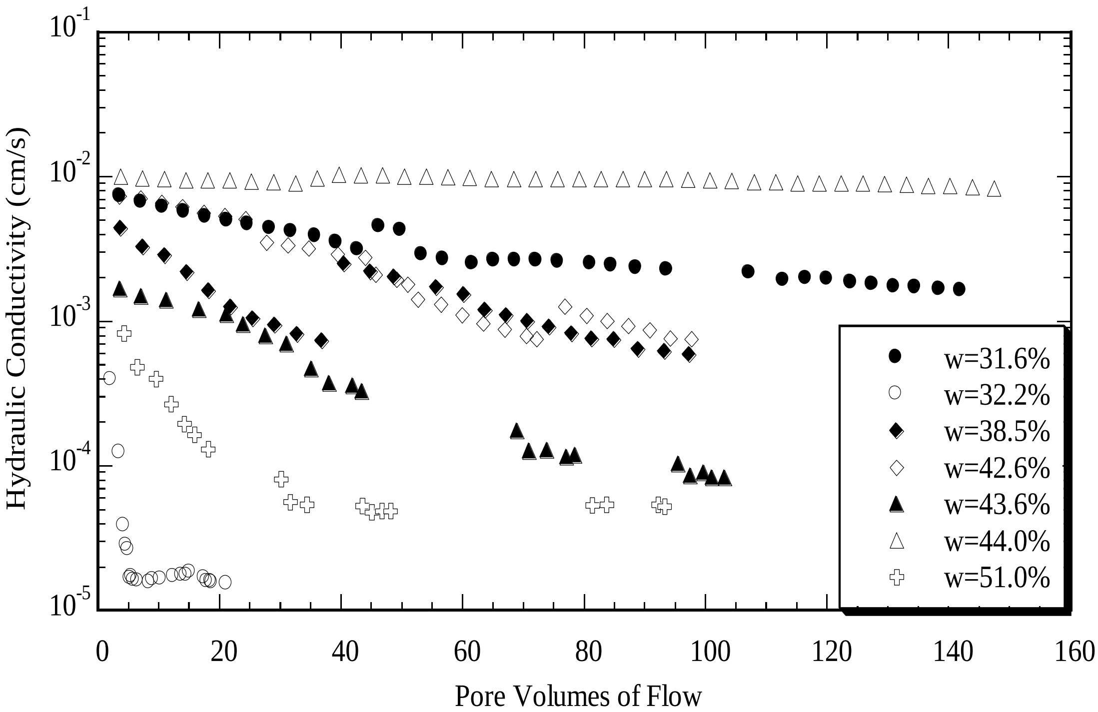

Figure 4.14 Hydraulic conductivity behavior of GZ-2

Table 4.6 Hydraulic conductivity of GZ-2 at various water contents

Sample No	w %	γ_d	k_{final} (cm /s)
1	31.6	1.01	1.65×10^{-3}
2	32.3	0.98	1.55×10^{-5}
3	38.5	1.04	6.05×10^{-4}
4*	42.6	0.98	7.63×10^{-4}
5*	43.6	0.99	7.59×10^{-5}
6	44.1	1.03	4.82×10^{-3}
7	51.4	1.02	5.30×10^{-5}

* Far from the standard Proctor compaction curve (represented with red squares)

As seen in Figure 4.14 and Table 4.6, hydraulic conductivity values of GZ-2 changed within the range of 1.55×10^{-5} - 4.82×10^{-3} cm/s.

The hydraulic conductivities of GZ-1 and GZ-2 were stable throughout the test duration when they had compaction water contents between 44% and 45.5%. The hydraulic conductivities of three tests (two for GZ-1 and one for GZ-2) were within the range of 1×10^{-2} - 2×10^{-3} cm/s. This may address possible side-wall leakage while testing with rigid–wall permeameters. This is because that the samples compacted at similar water contents (i.e. 45.9% and 43.6% for GZ-1 and GZ-2, respectively) had about two orders of magnitude less hydraulic conductivities than these three values as shown in Figure 4.12 and Figure 4.14.

Although there is no comprehensive study on hydraulic conductivity behavior of zeolites, Park at al., (2002) performed hydraulic conductivity tests with flexible-wall permeameter under the overburden soil pressure. They reported that the 100% clinoptilolite sample's (with 0-1 mm particle size) hydraulic conductivity was around 1×10^{-6} cm/s. The reported values are significantly lower than obtained results in this study. The difference between this study and Park et. al. (2002) may be attributed to the sample preparation methods or the difference in the testing methods. They poured the samples into the mold and they did not apply any compaction energy, while they were preparing their specimens. Also specific gravity of the clinoptilolite which was used in the study of Park et. al. (2002) is (2.16) less than the specific gravities of zeolites in this study (2.34).

4.5.2 Falling Head Hydraulic Conductivity Test Results

The hydraulic conductivity of compacted fine zeolites at various water contents are shown in terms of PVFs. Hydraulic conductivity test results for FZ-1 and FZ-2 are shown in Figure 4.15 a-e and Figure 4.18 a-d, respectively. Figure 4.15 a-e indicates the hydraulic conductivity test results of FZ-1 in terms of PVFs. In addition to this, outflow over inflow (Q_{out}/Q_{in}) ratios are also shown in these figures.

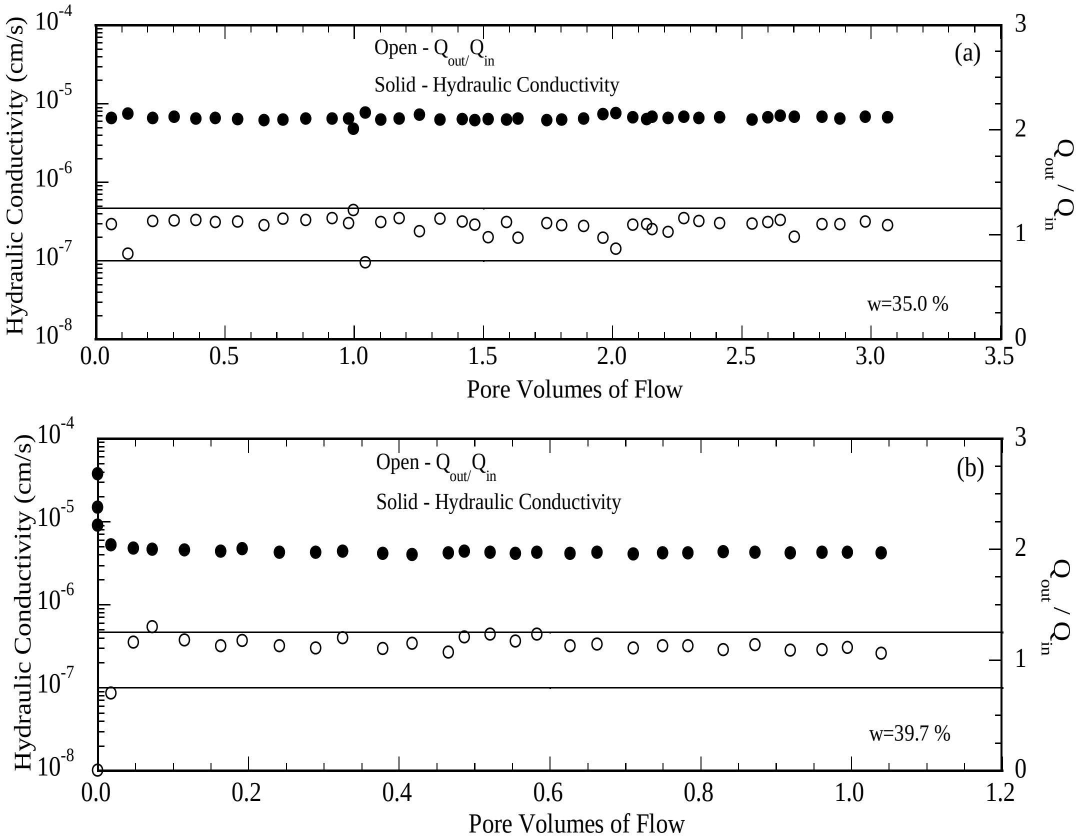

Figure 4.15 Hydraulic conductivity test results of FZ-1

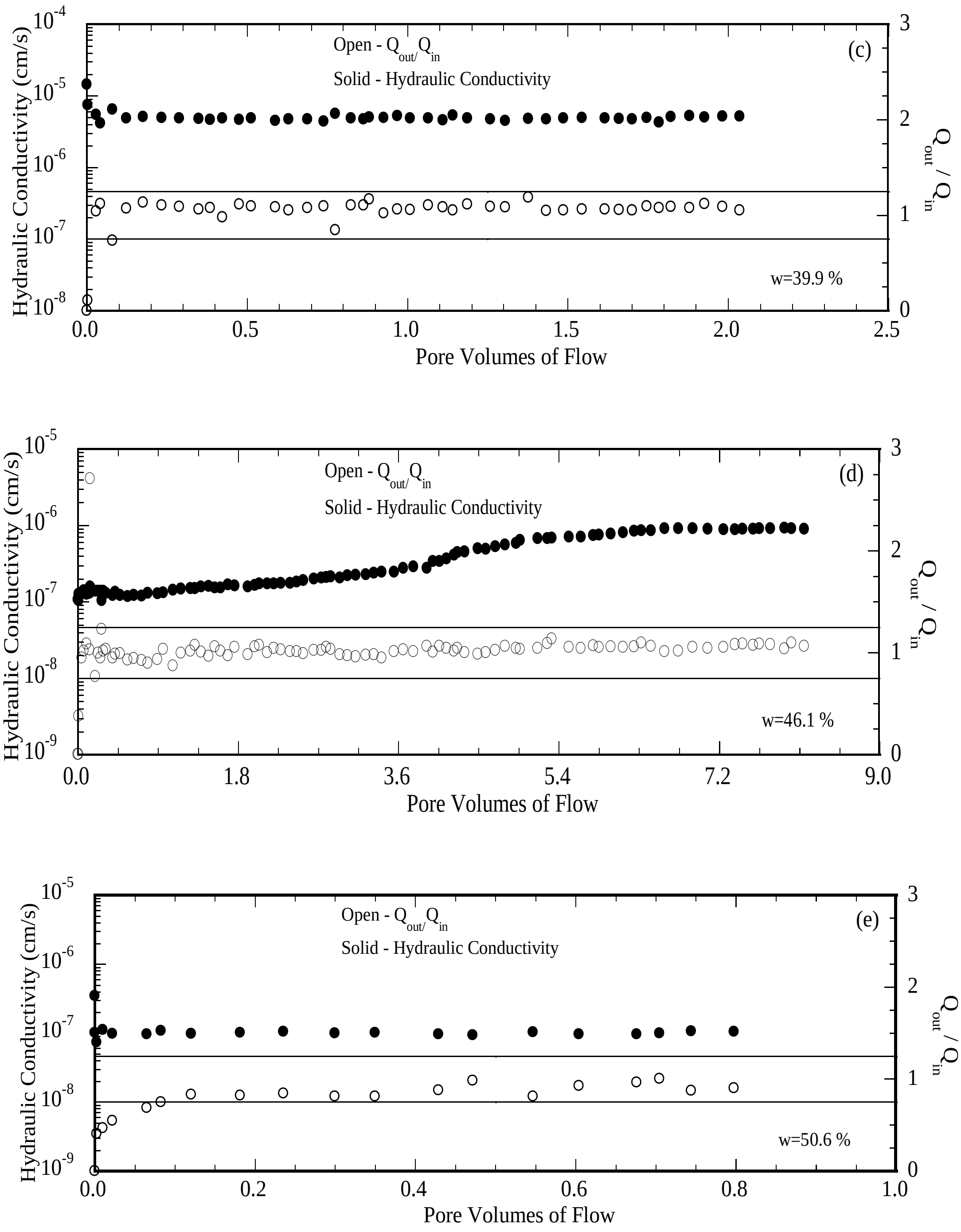

Figure 4.15 continued.

As seen in Figure 4.15 a, b, c and e, hydraulic conductivity values of FZ-1 were almost constant during the tests. The only exception occurs for the sample which was subjected to long term hydraulic conductivity at optimum water content. Even though the outflow over inflow (Q_{out}/Q_{in}) ratios were within the range of 0.75 and

1.25, hydraulic conductivity values started to increase after about 2 PVFs passed through the sample. Hydraulic conductivity of the specimen was increased from 1.64×10^{-7} cm/s to 8.94×10^{-7} cm/s.

In addition to this, falling head hydraulic conductivity tests required minimum one day and maximum 2.5 days at the dry sides of the optimum water content for FZ-1 (Figure 4.16a). Hydraulic conductivity variations of FZ-1 are also shown as a function of day in Figure 4.16 a-b. Figure 4.16a represents the hydraulic conductivity variation of FZ-1 at water contents less than optimum water content. Hydraulic conductivity variations of FZ-1 at or above optimum water contents are also illustrated in Figure 4.16b.

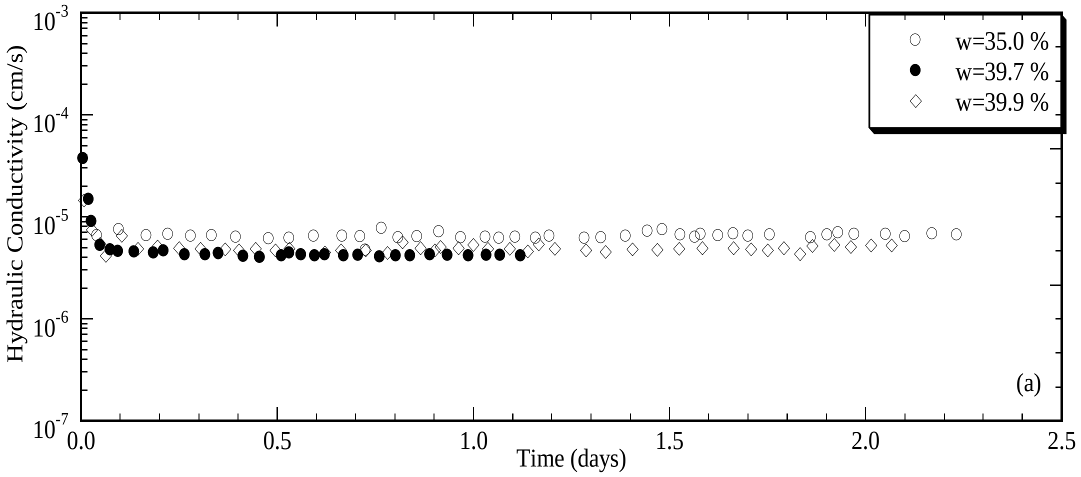

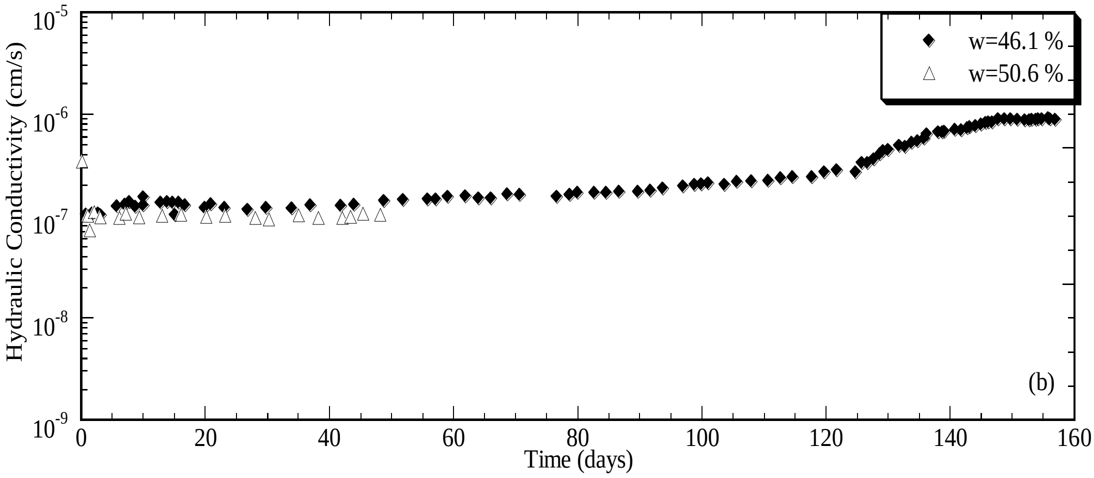

Figure 4.16 Variation of the hydraulic conductivity values of FZ-1 with time

As seen in Figure 4.16b, hydraulic conductivity tests of FZ-1 at optimum water content was terminated at the end of 5.5 months. The time required for the hydraulic stability of FZ-1 at the wet side of the optimum water content was about 50 days. All hydraulic conductivity test results are shown in Figure 4.17. Also, final hydraulic conductivity values are summarized in Table 4.7 as well.

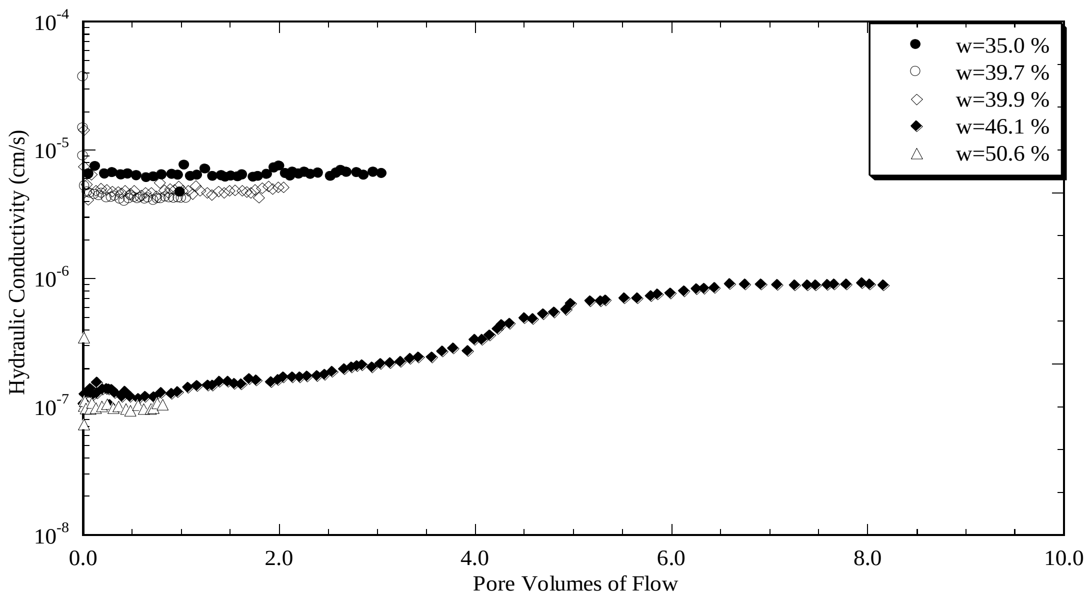

Figure 4.17 Hydraulic conductivity behavior of FZ-1

Table 4.7 Hydraulic conductivity of FZ-1 at various water contents

Sample No	w %	γ_d	k_{final} (cm /s)
1	35.0	1.02	6.73×10^{-6}
2	39.7	1.04	4.18×10^{-6}
3	39.9	1.03	4.83×10^{-6}
4	46.1	1.08	1.56×10^{-7}
5	50.6	1.04	1.05×10^{-7}

As seen in Figure 4.17 and Table 4.7, hydraulic conductivity values of FZ-1 at the dry side of optimum water content are about $7x10^{-6}$ cm/s. However, at the optimum water content and the wet side of the optimum water content, hydraulic conductivity values decreased about one order of magnitude. Furthermore, hydraulic conductivity test results are shown in Figure 4.18 a-d for FZ-2.

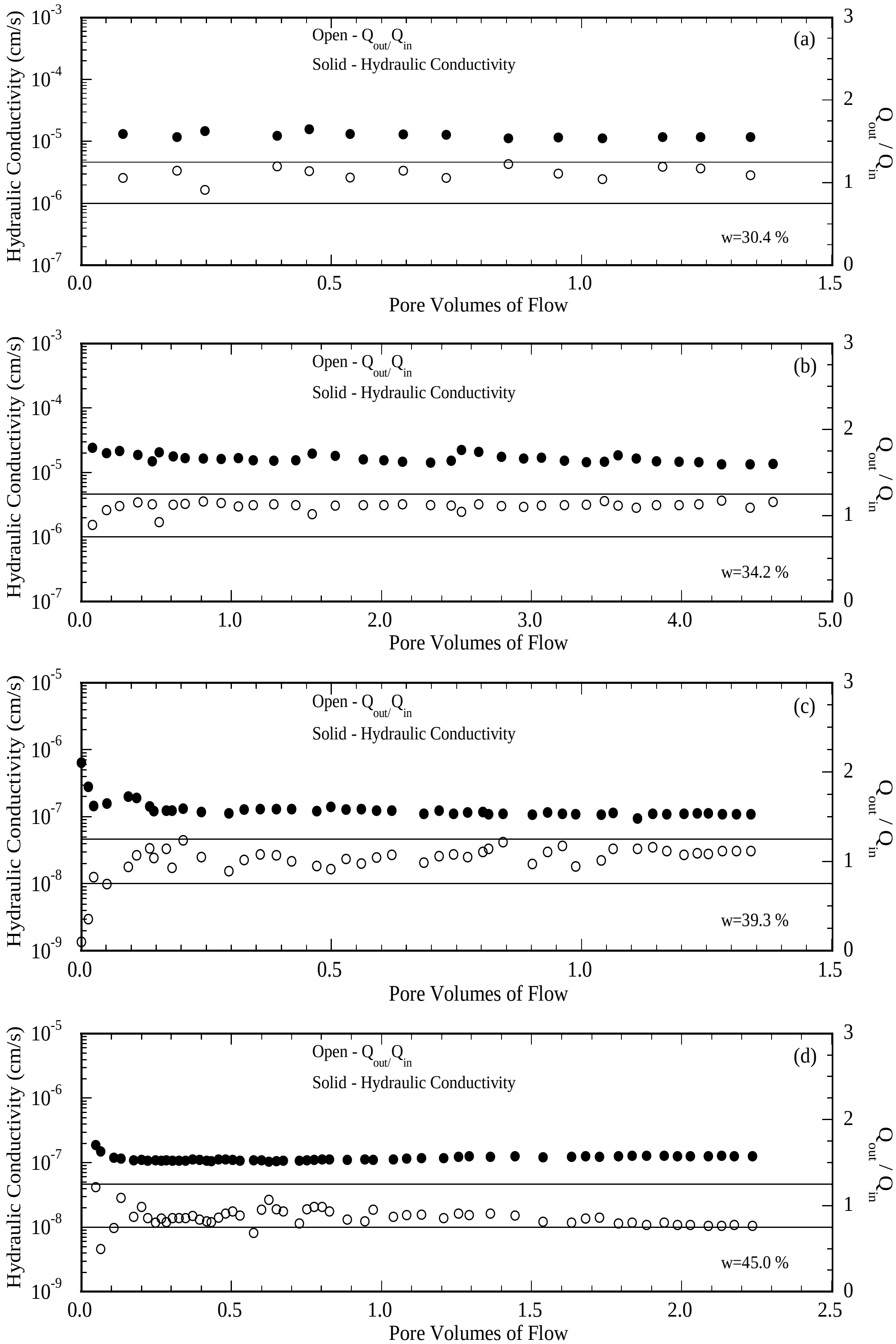

Figure 4.18 Hydraulic conductivity test results of FZ-2

As seen in Figure 4.18 a-d, hydraulic conductivity values of FZ-2 decreased maximum 6 times in comparison to the initial hydraulic conductivities and then keeps almost constant during the tests. All hydraulic conductivity test results are shown in Figure 4.19. Also, final hydraulic conductivity values are summarized in Table 4.8.

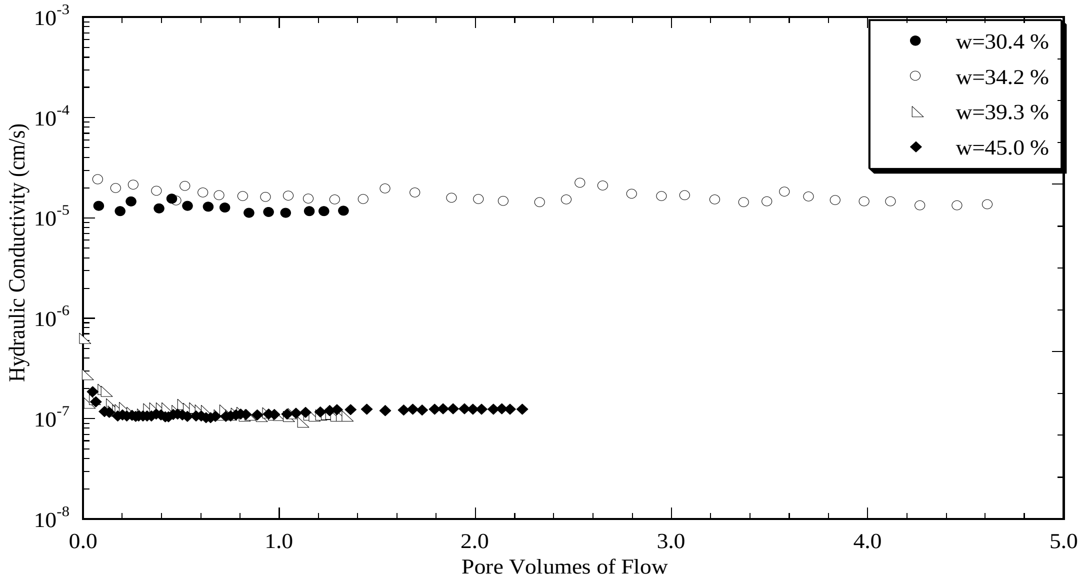

Figure 4.19 Hydraulic conductivity behavior of FZ-2

Table 4.8 Hydraulic conductivity of FZ-2 at various water contents

Sample No	w %	γ_d	k_{final} (cm /s)
1	30.4	1.17	1.16×10^{-5}
2	34.2	1.15	1.34×10^{-5}
3	39.3	1.19	1.06×10^{-7}
4	45.0	1.14	1.24×10^{-7}

According to the obtained results at the dry side of optimum water content for FZ-2, hydraulic conductivity values are about $1x10^{-5}$ cm/s. However, these values decreased about two orders of magnitude when the compaction optimum water content was at or above the optimum water content.

Also, long term hydraulic conductivity test results of fine zeolites are shown in Figure 4.20.

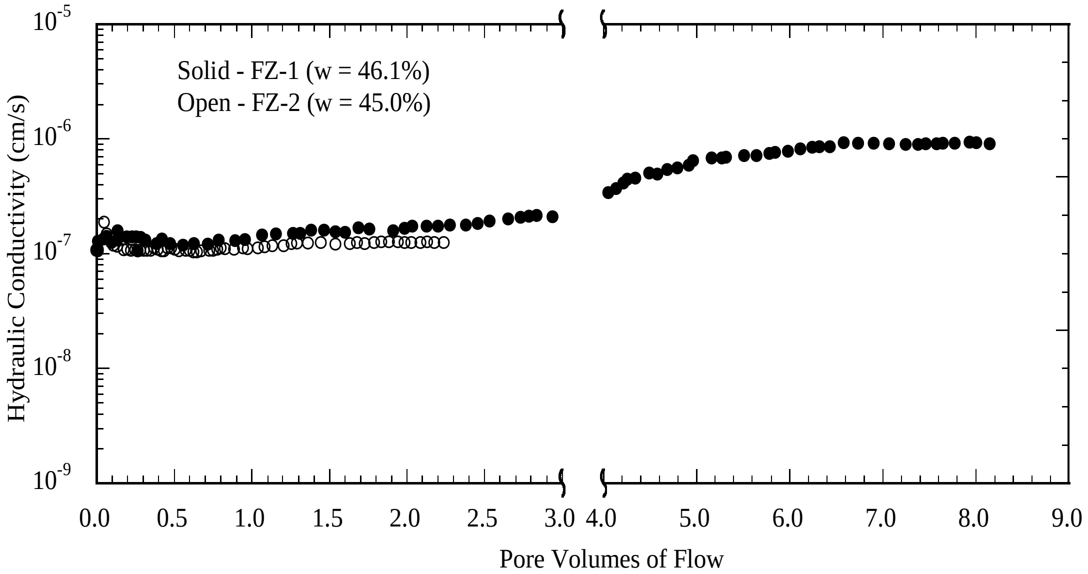

Figure 4.20 Long term hydraulic conductivity behavior

As seen in Figure 4.20, hydraulic conductivity of FZ-1 started to increase at 2 PVFs. This increment in hydraulic conductivity continued until 8.5 PVFs. Similar trend is also seen for FZ-2. However, due to the time restriction FZ-2's hydraulic conductivity test was terminated at 2.2 PVFs.

The relationship between fine content and hydraulic conductivity at optimum water content is given in Figure 4.21. One data from literature is also included in Figure 4.21 (Navia et al., 2005). As can be seen from Figure 4.21, there are two tests conducted on GZ-2 which had 5% fine content. For the first test, the hydraulic conductivity was obtained 7.6×10^{-5} cm/s. However, the hydraulic conductivity for the second test was about two orders of magnitude more than that of the first test (i.e. 4.8×10^{-3} cm/s). This difference may be due to the side-wall leakage that could be happened when the second test was running.

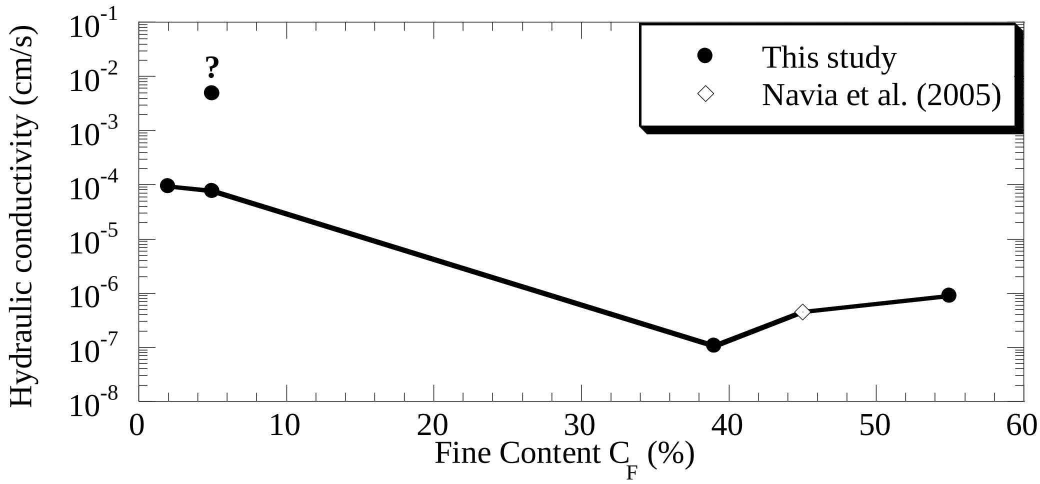

Figure 4.21 Hydraulic conductivity versus fine content relationship

In fact, hydraulic conductivity of zeolite decreased about three orders of magnitude up to 40% fine content. The fine content below 40% may not enough to clog the pores. Moreover, zeolite fine particles may be eroded between the granular particles which led to increase the hydraulic conductivity. This was also confirmed with my observation while running the test. At the very beginning of the test, the outflow water was blurred with the eroded zeolite particles and then the outflow became limpid while the test was running (Figure 4.22 a-b). Between 40% and 55% fine content, hydraulic conductivity increased about 10-fold. The literature data corresponds well with the findings of this study. Thus, it can be stated that the hydraulic conductivity of compacted zeolite is between 1×10^{-6} and 1×10^{-7} cm/s when the fine content was within the range of 40-55%.

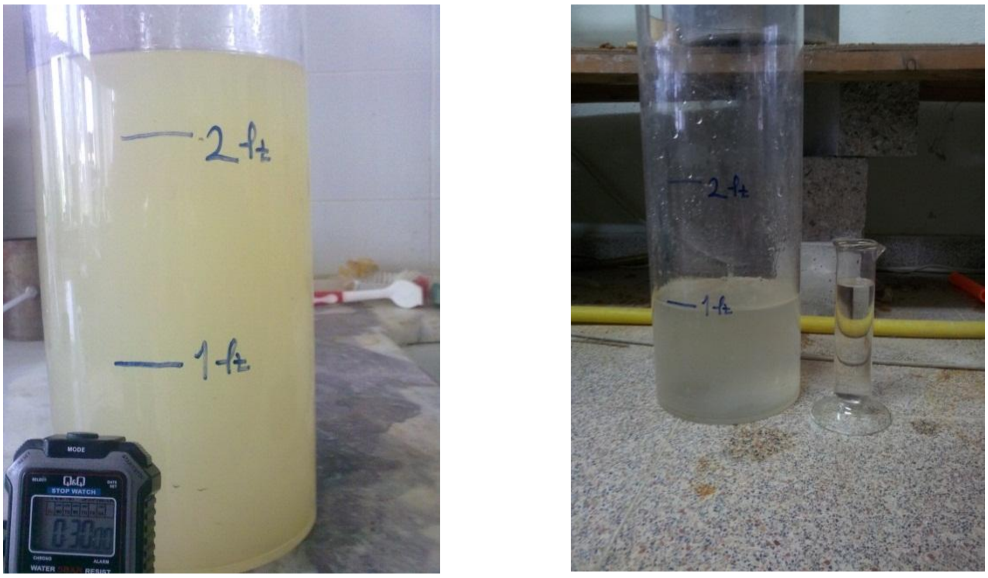

Figure 4.22 Outflow water at the beginning of the hydraulic conductivity tests

The relationship between hydraulic conductivity and compaction water content is shown in Figure 4.23. Two samples of GZ-2 that were compacted at optimum water content but had lower dry densities are represented with red solid squares in the same figure.

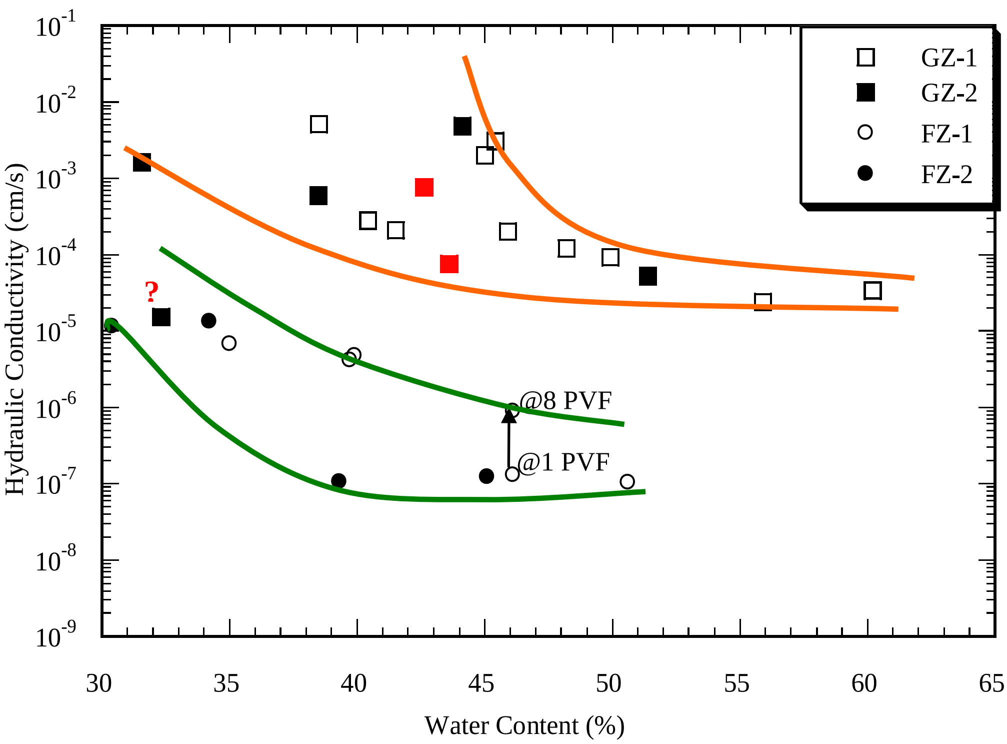

Figure 4.23 Hydraulic conductivity behaviors of compacted granular and fine zeolites

A decreasing trend of hydraulic conductivity with increasing compaction water content exists in Figure 4.23. These specimens that compacted at dry side of optimum generally have higher hydraulic conductivity. One point was out of this order. It may be an experimental error. Although long term hydraulic conductivity of FZ-1 increased about one order of magnitude, it is still less than the hydraulic conductivity of granular zeolites.

In addition to this, the relationship between hydraulic conductivity and maximum dry unit weight is also shown in Figure 4.24. Similar to Figure 4.23, two samples of GZ-2 are also represented with red solid squares in the Figure 4.24.

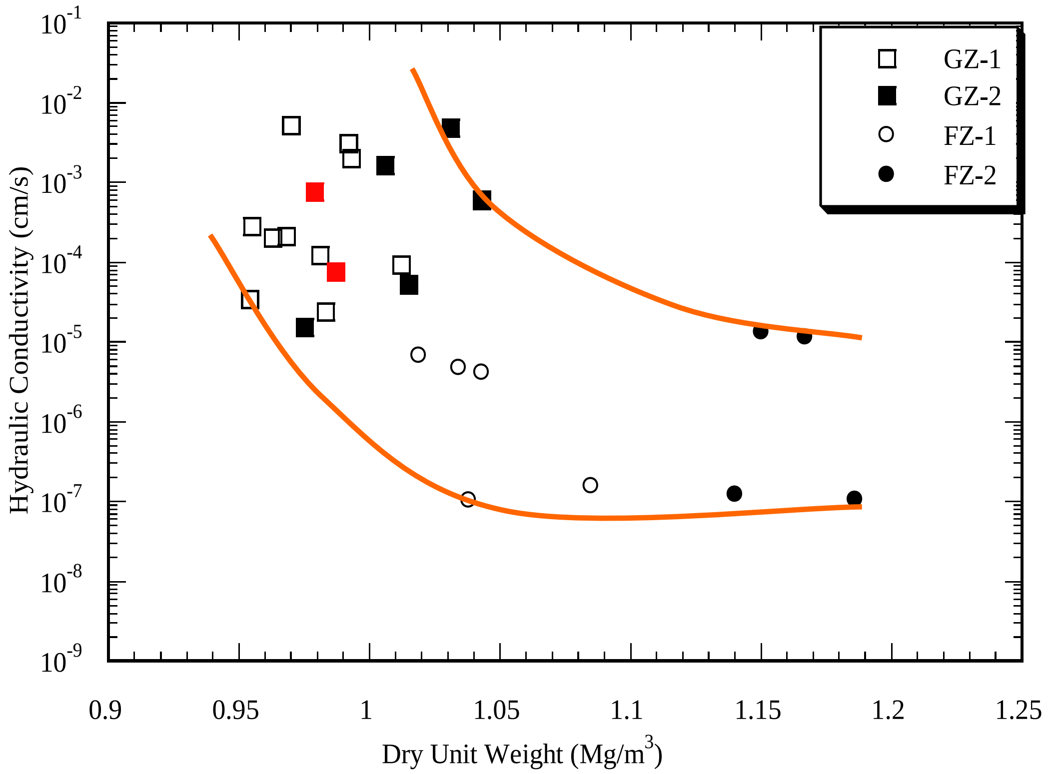

Figure 4.24 Hydraulic conductivity behaviors of compacted granular and fine zeolites

As seen in Figure 4.24, such decreasing trend between hydraulic conductivity and compaction water content does not exist between hydraulic conductivity and maximum dry unit weight for any of compacted zeolites. However, when all the hydraulic conductivity results evaluated together, it is seen that increase in the dry unit weight results in a decrease in hydraulic conductivity. In other words, decrease in the particle size lead to decrease the hydraulic conductivity. This may be attributed to the lower dry unit weights of granular zeolites. As mentioned before while the particle size increases, voids in the specimens increase as well. Thus, increase in the voids lead to decrease the dry unit weights. Representation of hydraulic conductivity and dry unit weight relationship in terms of void ratio is also shown in Figure 4.25. It is clear that there is an increasing trend between void ratio (e) and hydraulic conductivity (Figure 4.25). As a result, increase in the void ratio lead to increase the hydraulic conductivity.

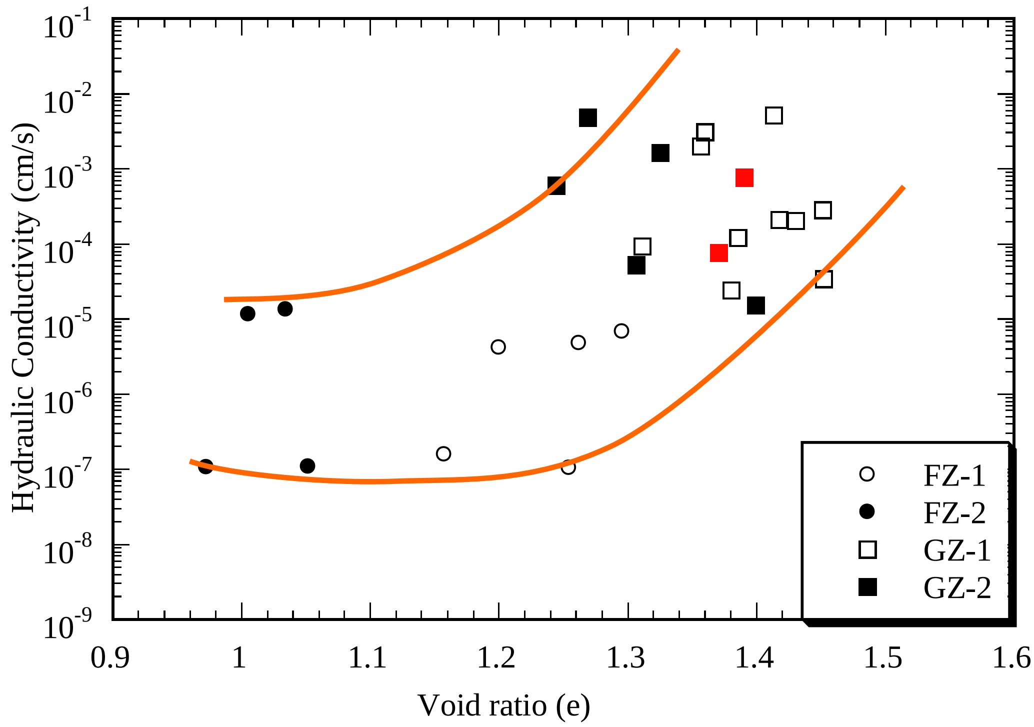

Figure 4.25 Hydraulic conductivity behaviors of compacted granular and fine zeolites

CHAPTER FIVE
CONCLUSIONS AND RECOMMENDATIONS

In the content of this thesis, the summary of the results are given below:

- Compacted fine zeolites had higher maximum dry unit weights (γ_{dmax}) and lower optimum water contents than compacted granular zeolites.

- The maximum dry unit weights (γ_{dmax}) of compacted zeolites are significantly less than the maximum dry unit weights (γ_{dmax}) of compacted sands and clays.

- Although compacted granular zeolites have no cohesion intercepts, 0.291 kg/cm^2 and 0.211 kg/cm^2 cohesion intercept values were obtained for FZ-1 and FZ-2, respectively.

- Increase in the zeolite particle size lead to increase the internal friction angel (ϕ').

- The peak shear strengths of compacted zeolites are comparable to those of dense sands.

- Although FZ-1 had lower maximum dry unit weight (γ_{dmax}) than FZ-2, the unconfined compressive strength of FZ-1 is higher than the unconfined compressive strength of FZ-2. This may be attributed to the higher fine content for FZ-1 than for FZ-2 (55% vs. 39%).

- The hydraulic conductivity of FZ-1 at optimum water content increase about seven times during the long term hydraulic conductivity testing (i.e 5.5 months). This may be attributed from side-wall leakage or water may be started to pass through the intergranular pores.

- There is a decreasing trend between hydraulic conductivity and compaction water content for all tested compacted zeolites. Increase in the compaction water content lead to decrease the hydraulic conductivity.

- Such decreasing trend is not observed between maximum dry unit weight (γ_{dmax}) and hydraulic conductivity for neither of compacted zeolites. However, when the hydraulic conductivities of zeolites are assessed together, it is seen that increase in the dry unit weight (γ_{dmax}) result in a decrease in the hydraulic conductivity.

The geotechnical characterization of zeolites should be investigated with further studies. Based on the obtained results, the following recommendations are proposed:

- It is already determined that shear strength properties of compacted zeolites are comparable to dense sands. Also, maximum dry unit weight (γ_{dmax}) of zeolites are significantly less than those of sands and clay. This is an important advantage during the construction when the settlements have critical importance. In this situation, zeolites may be used instead of sand and clays as a lightweight geomaterial.

- The long term hydraulic conductivity of zeolites has not been investigated in detail. In order to determine the long term hydraulic conductivity of zeolites, the number of tests should be increased. Also, several hydraulic conductivity tests should be performed with back pressures in order to obtain the fully saturated samples.

- It's generally accepted that the hydraulic conductivity of compacted soil liners and covers should be less than or equal to $1x10^{-7}$ cm/s. Variation of the hydraulic conductivities of zeolites were in the range of $2x10^{-3}$ cm/s and $1x10^{-7}$ cm/s. Since lower hydraulic conductivity values were not achieved, it’s not recommended to use tested zeolites alone for a compacted soil liner.

REFERENCES

ASTM D 422; Standard test method for particle-size analysis of soils, *The American Society for Testing and Materials*, West Conshohocken, United States (2007).

ASTM D 4318-10; Standard test methods for liquid limit, plastic limit, and plasticity index of soils, *The American Society for Testing and Materials*, West Conshohocken, United States (2010).

ASTM D 854-10; Standard test methods for specific gravity of soil solids by water pycnometer, *The American Society for Testing and Materials*, West Conshohocken, United States (2010).

ASTM D 698-07; Standard test methods for laboratory compaction characteristics of soil using standard effort (12,400 ft-lbf/ft^3(600 kN-m/m^3)), *The American Society for Testing and Materials*, West Conshohocken, United States (2012).

ASTM D2435/D2435M – 11; Standard test methods for one-dimensional consolidation properties of soils using incremental loading, *The American Society for Testing and Materials*, West Conshohocken, United States (2011).

ASTM D3080/D3080M – 11; Standard test methods for direct shear test of soils under consolidated drained conditions, *The American Society for Testing and Materials*, West Conshohocken, United States (2012).

ASTM D 2166-06; Standard test methods for unconfined compressive strength of cohesive soil, *The American Society for Testing and Materials*, West Conshohocken, United States (2007).

ASTM D 5696 - 96; Standard guide for sampling strategies for heterogeneous wastes, *The American Society for Testing and Materials*, West Conshohocken, United States (2006).

Blenchard, G., Maunaye, M., & Martin, G. (1984). Removal of heavy metals from waters by means of natural zeolites. *Water Research, 18 (12),* 1501-1507.

Birsoy, R. (2002). Activity diagrams of zeolites: implications for the occurances of zeolites in Turkey and of eronite wordwide. *Clays and Clay Minerals, 50*, 136-144.

Colella, C. (2007). Natural zeolites and environment. In J. C. H. Bekkum, A. Corma, & F. Schüth, (Ed.). *Introduction to Zeolite Science and Practice* (3rd Revised ed.) (999-1035). Amsterdam: Elsevier B.V.

Crystal healing definition. (n.d.) Retrieved June 20, 2012, from http://www.crystalflame.com/en/crystal-healing-info/what-quartz-made/

Daniel, D.E. (1994). State-of-art: Laboratory hydraulic conductivity tests for saturated soils. In the *Hydraulic conductivity and waste contaminant transport in soil STP 1142, ASTM,* Philadelphia, 30-78.

Güney, Y., & Koyuncu, H. (2002). The behavior of bentonite-zeolite landfill versus salt and metal pollution. *6th İnter. Symp. On Environmental Geotechnology and Grobal Sustainable Development,* Seoul: Hong.

Holtz, R.D., Kovacs, W.D. & Sheahan, T.C. (2011). An Introduction to Geotechnical Engineering (2nd ed.).

Howell, J. L., Shackelford, C.D., Amer, N. H., & Stern, R. T. (1997). Compaction of sand-processed clay soil mixtures. *Geotechnical Testing Journal, 20* (4), 443-458.

Jacobs, P.H., & Forstner, U. (1999). Concept of sub-aqueous capping of contaminated sediments with active barrier systems using natural and modified zeolites. *Water Research, 33* (9), 2083-2087.

Kaçmaz, H., & Köktürk, U. (2004). Geochemistry and mineralogy of zeolitic tuffs from the Alaçatı (Çeşme) area, Turkey. *Clays and Clay Minerals, 52*, 705-713.

Kaya, A., & Durukan, S. (2004). Utilization of bentonite-embedded zeolite as clay liner. *Applied Clay Science, 25,* 83-91.

Kayabalı, K. (1997). Engineering aspects of a novel landfill liner material: bentonite-amended natural zeolite. *Engineering Geology, 46*, 105-114.

Koyama, K. & Takeuchi, Y. (1977). Clinoptilolite: the distribution of potassium atoms and its role in thermal stability. *Z. Kristallogr., 145,* 216-239.

Koizumi, M. & Roy, R. (1960). Zeolite studies. I. Synthesis and stability of calcium zeolites. *J. Geol., 68,* 41-53.

Köktürk, U. (1995). Zeolit madenciliği ve çevre sağlığına etkileri. *Endüstriyel hammaddeler sempozyumu,* İzmir, 21-22 April 1995.

Lee, S. H., Jo, H. Y., Yun, S. T., & Lee, Y. J. (2010). Evaluation of Factors Affecting Performance of Zeolitic Rock Barrier to Remove Zinc From Waterç *Journal of Hazardous Materials,* HAZMAT-10726.

Maesen, T. (2007). The zeolite scene – An overview. In J. C. H. Bekkum, A. Corma, & F. Schüth, (Eds.). *Introduction to Zeolite Science and Practice* (3rd Revised ed.) (1-12). Amsterdam: Elsevier B.V.

Masters, A.F & Maschmeyer, T. (2010). Zeolites – From curiosity to cornerstone. In M. Stöckher, (Ed.). *Microporous and Mesoporous Materials* Vol.142 (423-438). Sydney: Elsevier B.V.

Mumpton, F. A. (1999). La roca magica: Uses of natural zeolites in agriculture and industry. *Proc. Natl. Acad. Sci. 96,* 3463-3470.

Navia, R., Hafner, G., Raber, G., Lorber, K. E., Schöffmann, E., & Vortisch, W. (2005). The use of volcanic soil as mineral landfill liner – I. Physicochemical characterization and comparison with zeolites. *Waste Manage Res., 23,* 249-259.

Ölmez, A. (2007). Determination of compaction parameters by mens of regression approaches. *Master's thesis*. Niğde, August 2007.

Ören, A.H. (2007). Engineering investigation of zeolite-bentonite mixtures for landfill liner appications. *Master's thesis*. İzmir, May 2007.

Ören, A. H., Kaya, A., & Kayalar, A. S. (2011). Hydraulic conductivity of zeolite-bentonite mixtures in comparison with sand-bentonite mixtures. *Canadian Geotechnical Journal, 48* (9), 1343-1353.

Park, J. B., Lee, S. H., Lee, J. W., & Lee, C. Y. (2002). Lab scale experiments for permeable reactive barriers against contaminated groundwater with ammonium and heavy metals using clinoptilolite. *Journal of Hazardous Materials, 95,* 65-79.

Shaqour, F., Whit, S., & Webb, J. (2011). Geotechnical characterization of geomaterial blends with zeolitic tuffs for use as landfill liners. *Bull Eng. Geol. Environ, 70,* 691-697.

Sridharan, A., & Sivapullaiah, P.V. (2005). Mini compaction test apparatus for fine grained soils. *ASTM Journal of Testing and Evaluation, 28*, 240-246.

Structure-adaptive materials prediction. (n.d.) Retrieved May 15, 2012, from http://www.cmasc.gmu.edu/samp.htm

Trgo, M., & Peric J. (2003). Interaction of the zeolitic tuff with Zn-containing simulated pollutant solutions. *Journal of Colloid and Interface Science*, *260*, 166-175.

Yuan, G. (1997). Zeolite and high carbon fly ash mixes as liner materials for lead/phenol sorption. *Master's thesis*. Newfoundland, May 1997.

Yükselen-Aksoy, Y. (2010). Characterization of two natural zeolites for geotechnical and geoenvironmental applications. *Applied Clay Science*, *50*, 130-136.